

THE PENNSYLVANIA STATE UNIVERSITY
SCHREYER HONORS COLLEGE

DEPARTMENT OF BIOCHEMISTRY AND MOLECULAR BIOLOGY

SYNTHESIS, EFFICACY, AND MOLECULAR TARGETING OF HYDRAZIDE
CLASS *TRANS*-TRANSLATION INHIBITORS

GREGORY HUNTER BABUNOVIC
SPRING 2015

A thesis
submitted in partial fulfillment
of the requirements
for baccalaureate degrees
in Microbiology and Immunology and Infectious Disease
with honors in Microbiology

Reviewed and approved* by the following:

Kenneth Keiler
Associate Professor of Biochemistry and Molecular Biology
Thesis Supervisor

Sarah Ades
Associate Professor of Biochemistry and Molecular Biology
Honors Adviser

Scott Selleck
Professor and Department Head for Biochemistry and Molecular Biology

* Signatures are on file in the Schreyer Honors College.

ABSTRACT

Antibiotic resistance is a serious and growing problem in the modern world, and the discovery and characterization of novel antimicrobials is a top priority. *Trans*-translation, a conserved and oftentimes essential ribosome-rescue process in bacteria, is a promising target for novel antibacterial drugs. A high-throughput screening assay for the *in vivo* inhibition of *trans*-translation identified several molecular classes of compounds that potently inhibit this pathway; members of these classes have shown antibiotic activity against pathogenic and nonpathogenic bacteria. Here, various members of a novel class of *trans*-translation inhibitors with an acyl hydrazide-thiol-amide substructure were synthesized and tested for antibiotic activity against both pathogenic and nonpathogenic bacteria. An inhibitor with confirmed antibiotic efficacy was used in combination with other known inhibitors of *trans*-translation and was found to have additive effects with members of the oxadiazole class, implying a related molecular target. A molecular probe for the novel class of inhibitors was synthesized and used in a click chemistry-based assay to identify protein binding partners of this class of compounds within bacterial lysates. The click chemistry-based assay identified a protein of approximately 25 kDa that appears to be selectively bound by this probe; this protein is only bound in lysates containing accumulated stalled non-stop ribosomal complexes that are substrates for the *trans*-translation reaction. Future studies will seek to validate this result and investigate whether this protein is a target of the novel inhibitor class.

TABLE OF CONTENTS

LIST OF FIGURES.....	iii
LIST OF TABLES.....	iv
ACKNOWLEDGEMENTS	V
INTRODUCTION.....	1
<i>Trans</i> -Translation as an Antibiotic Target.....	1
High-Throughput Screen for <i>trans</i> -Translation Inhibitors	3
The Hydrazide Class of <i>trans</i> -Translation Inhibitors	5
MATERIALS AND METHODS	8
Reagents, Strains, and Media	8
Synthesis of KKL-64.....	9
Synthesis of KKL-588.....	9
Synthesis of 4-Phenylbenzoic Hydrazide	10
Synthesis of KKL-63.....	10
Minimum Inhibitory Concentration (MIC) Broth Microdilution Assays.....	11
Combination Activity Checkerboard Assays	11
Click Chemistry Conjugation Assay for Target Identification.....	12
RESULTS.....	14
Synthesis of Hydrazide Class Inhibitors	14
Hydrazide Class Inhibitors are Effective Antibiotics	20
Combinatorial Activity of Hydrazide Class and Other Inhibitors	22
Click Chemistry Probe Assay for Hydrazide Inhibitor Targets.....	26
DISCUSSION.....	33
REFERENCES.....	38
ACADEMIC VITA	

LIST OF FIGURES

Figure 1- The steps of trans-translation.....	2
Figure 2- Luciferase assay for the inhibition of <i>trans</i> -translation.....	4
Figure 3- Comparison of hydrazide and non-hydrazide class inhibitors.....	7
Figure 4- Synthetic schemes for hydrazide class inhibitors	15
Figure 5- Synthetic scheme for 4-phenylbenzoic hydrazide.....	15
Figure 6- Annotated proton NMR data for synthesized compounds.....	16
Figure 7- Activity of KKL-64 in combination with other <i>trans</i> -translation inhibitors	25
Figure 8- Chemical structures related to the KKL-2101 click probe assay	27
Figure 9- Click chemistry assay for the binding of the KKL-2101 hydrazide probe to target protein(s).....	29
Figure 10- UV illuminated gel with KKL-2101 probed samples	32

LIST OF TABLES

Table 1- Hydrazide class inhibitors identified by the high-throughput screen.....	6
Table 2- Media used for different bacterial strains.....	8
Table 3- Mean MIC values for synthesized hydrazide class inhibitors in nonpathogenic bacterial strains.....	21
Table 4- Mean MIC values for synthesized hydrazide class inhibitors in pathogenic bacterial strains.....	22

ACKNOWLEDGEMENTS

I would like to thank my thesis advisor, Dr. Kenneth Keiler, for accepting me into his lab three years ago and assisting my development as a scientist since then with both his resources and his guidance. I would also like to thank my honors advisor, Dr. Sarah Ades, for being able to work with me at any time and reading the roughest version of this thesis. Both Dr. Keiler and Dr. Ades were also supportive in their willingness to write letters of recommendation and their design and teaching of BMB 488 and MICRB 202, both of which were essential to my scientific growth. I owe a great deal to several more senior members of the Keiler Lab, including Dr. Nitya Ramadoss—who had the patience to help me adjust to my first semester performing research—and Dr. John Alumasa, whose constant assurances that the hydrazide project was “brilliant” were both calming and entertaining. Divya Hosangadi and Christopher Rae, the other undergraduates of the Keiler Lab Class of 2015, were both essential in my thesis process; Divya joined in the struggle against contamination early on, while Chris came in later and provided a set of ears for my more far-fetched models of what the inhibitors may be doing on a molecular level. I extend my gratitude to Heather Feaga for sparking the idea of using pNS-His in the click assay, and to all the members of the Keiler Lab for helping me every day with myriad reagents, solid advice, and positive outlooks. Finally, I want to thank my father for teaching me how to write and how to think, and my mother for teaching me how to love science and wear an “I love miRNA” shirt with pride.

INTRODUCTION

Antibiotic resistance is a growing problem in the modern world. Resistance genes exist for every clinical antibiotic used today and very few new drugs have come out of the pharmaceutical pipeline in recent decades (1). A 2014 report by the World Health Organization warned that a post-antibiotic era, where common injuries and bacterial infections could regain their pre-antibiotic lethal status, is a distinct possibility in the 21st century (2). This situation makes the discovery of new antimicrobial compounds a top priority.

***Trans*-Translation as an Antibiotic Target**

One promising technique in the search for new antibiotics is the use of novel inhibitors of important pathways that have not yet been targeted by existing drugs. *Trans*-translation is a ribosome-rescue mechanism that is conserved in all bacteria, and is essential for survival or virulence in many pathogenic species (3-5). This essentiality makes the pathway a promising target for novel antibacterial therapeutics.

The need for ribosome rescue in bacteria arises from the nature of the prokaryotic cell, where a lack of compartmental separation between transcription and translation allows the coupling of the two processes, with ribosomes commencing translation on mRNA molecules that are still in the process of being transcribed. The downside to this coupling is that there is no quality-control step between transcription

and translation, so ribosomes may translate faulty or truncated mRNA molecules. This reaction can result in a “stalled” translation complex, with a ribosome stuck at the end of an mRNA containing no stop codon (non-stop mRNA), unable to recruit canonical release factors for ribosome recycling. In *Escherichia coli*, each ribosome forms a stalled non-stop complex an average of ~5 times per cell cycle (6).

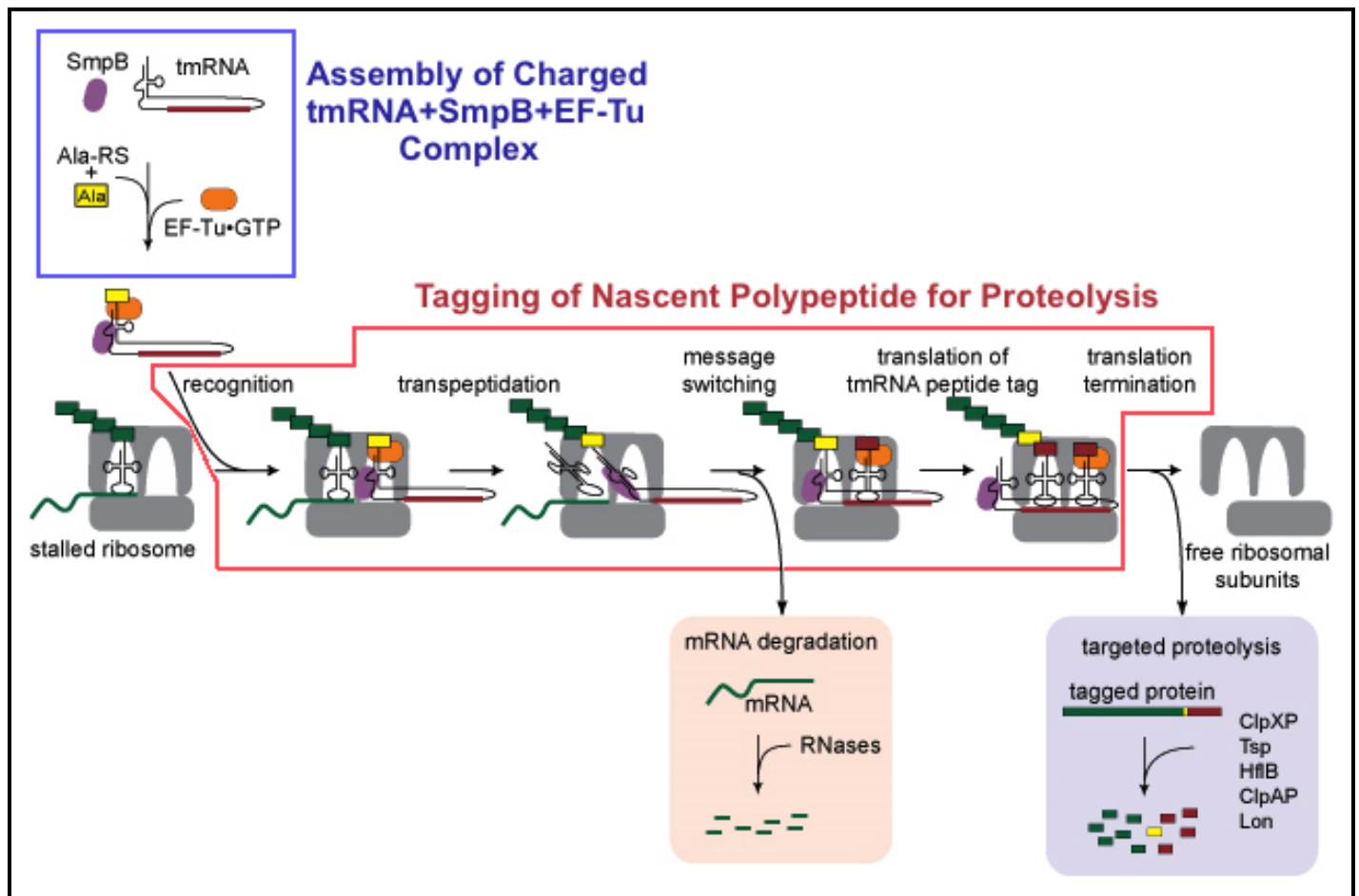


Figure 1- The steps of trans-translation

The *trans*-translation pathway begins with the association of SmpB, EF-Tu, and alanine with tmRNA. This assembly proceeds to act on stalled non-stop ribosomal complexes to remove faulty mRNA for degradation, add a proteolytic tag to the nascent polypeptide, and release the ribosomal subunits. Source: (7)

In *trans*-translation, the molecule tmRNA and its associated proteins SmpB and EF-Tu together resolve stalled ribosomes (Figure 1). tmRNA acts first as an aminoacyl-tRNA, recognizing the stalled non-stop complex and entering the A site of the ribosome to begin the transpeptidation process of adding its resident alanine to the nascent polypeptide chain (7). The molecule then acts as an mRNA, switching the message from the non-stop mRNA and coding for the remainder of an 11 amino acid C-terminal proteolytic tag. Following the translation of this tag, an encoded stop codon in the mRNA-like portion of tmRNA leads to the recruitment of canonical release factors for translation termination and the release of the ribosome and nascent protein. The previously translated faulty mRNA is destroyed by cellular RNases, while the nascent protein is degraded efficiently by several proteases including ClpXP, Tsp, and Lon (8,9).

High-Throughput Screen for *trans*-Translation Inhibitors

In collaboration with Novartis, the Keiler Lab designed and carried out a high-throughput screen (HTS) for the inhibition of *trans*-translation in *E. coli*. This screen tested the efficacy of compounds from a 663,000-member library using a luciferase reporter bacterial strain (10). The use of whole bacterial cells rather than an *in vitro* system was preferred due to the selection this method imparts towards compounds that can cross the bacterial cell membrane. The strain used carries an IPTG-inducible multicopy plasmid with a firefly luciferase gene (*luc*) containing the *trpAt* transcriptional terminator before the stop codon, resulting in abundant expression of non-stop *luc*

mRNA. These RNAs lead to ribosome stalling following the production of catalytically active luciferase protein. In bacteria where *trans*-translation is active this luciferase is tagged and proteolytically degraded, resulting in dark cells when luciferase substrate is added to the culture medium. Meanwhile, when *trans*-translation is inhibited the luciferase protein is not tagged or proteolytically degraded, and the cells become “bright” in terms of luminescence when substrate is added to the culture (Figure 2).

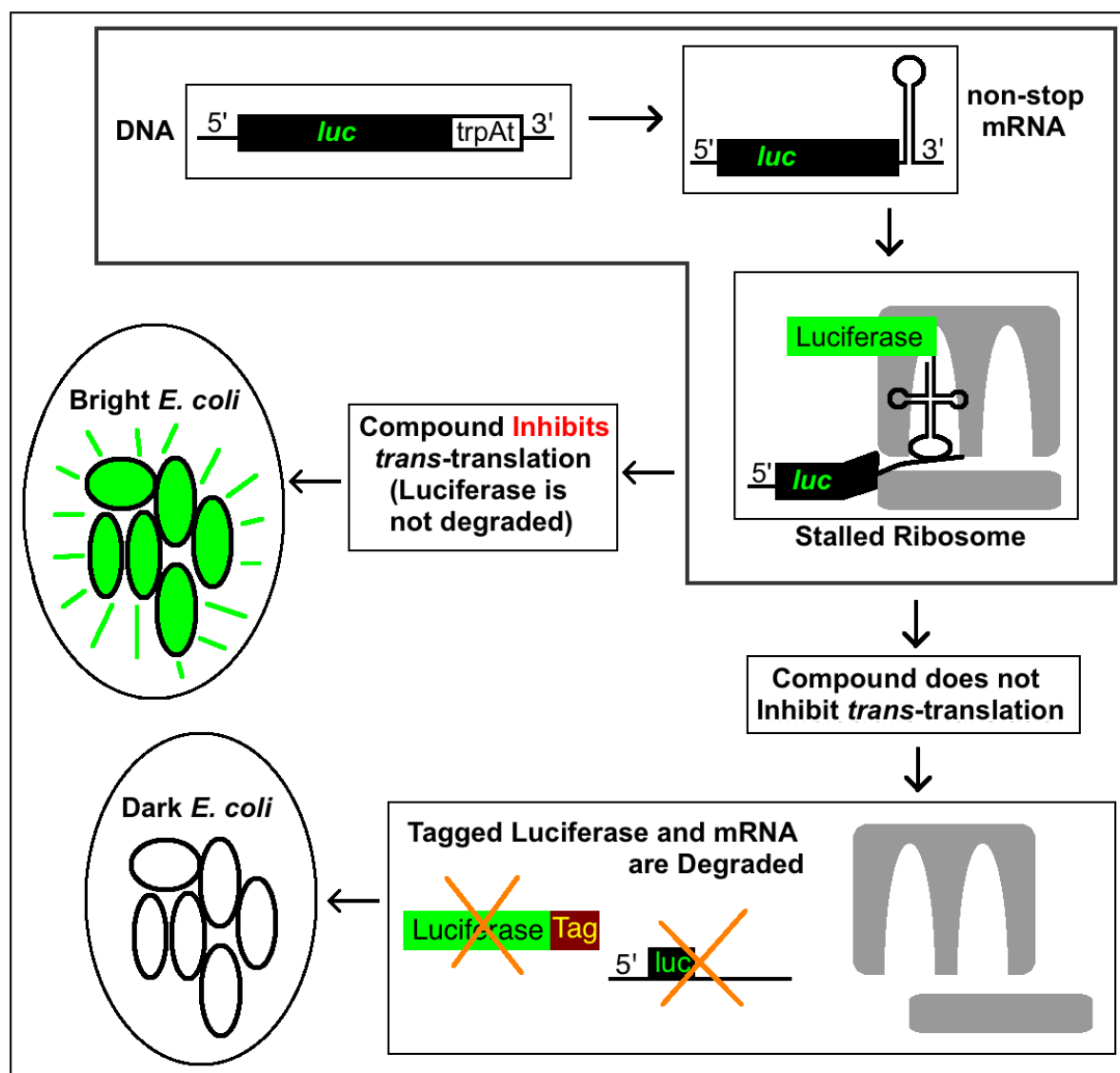


Figure 2- Luciferase assay for the inhibition of *trans*-translation

Non-stop *luc* mRNA produces stalled non-stop ribosomal complexes. In the presence of a functional *trans*-translation system, the complexes are resolved, the luciferase is tagged and degraded, and the addition of luciferase substrate does not produce luminescence. Cell-permeable inhibitors of *trans*-translation prevent the tagging and degradation of luciferase, so excess substrate results in >2-fold increase in luminescence at inhibitor concentration of 10 μ M.

With inhibition defined as a >2-fold increase in luminescence versus a vehicle control when compound is added at 10 μ M, the screen identified 178 compounds that inhibit *trans*-translation in *E. coli*. Of these hits, 46 compounds were selected for further study based on availability; many of these, such as the molecules KKL-35 and KKL-55, have since been extensively investigated and shown to be effective antibiotics (10). However, the other 132 compounds identified by the screen have not been studied in significant detail. This provides a unique opportunity for investigation of the underexplored potential of these molecules.

The Hydrazone Class of *trans*-Translation Inhibitors

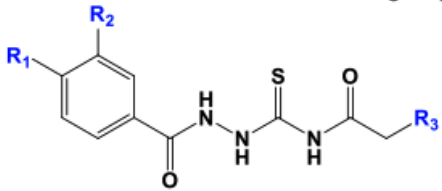
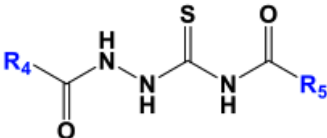
Within these 132 compounds, a group of inhibitors was identified with a conserved acyl hydrazone-thiol-amide substructure; this group is here on referred to as the “hydrazone” class of molecules. The screen identified 21 separate inhibitors that are members of the hydrazone class, indicating that the acyl hydrazone-thiol-amide substructure maintains activity with a wide variety of side groups (Table 1). These hydrazone class molecules are structurally distinct from representatives of the other characterized classes of *trans*-translation inhibitors (Figure 3).

For the completion of this thesis, several members of the hydrazone class of *trans*-translation inhibitors were synthesized and tested for antibiotic efficacy in a variety of pathogenic and nonpathogenic bacterial species. A member of the hydrazone class of compounds was tested in combination with other known inhibitors of *trans*-translation

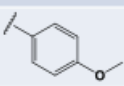
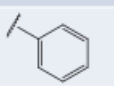
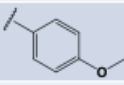
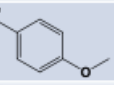
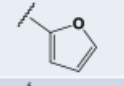
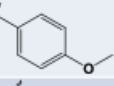
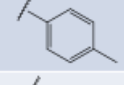
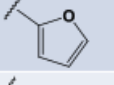
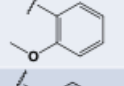
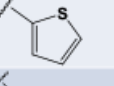
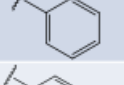
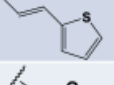
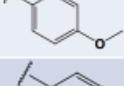
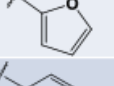
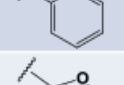
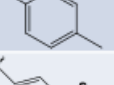
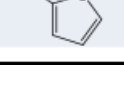
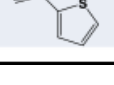
in a search for synergistic or additive effects. The insights from this combinatory approach informed the design of a novel assay to determine macromolecular binding partners of the hydrazide class of compounds. For this assay, an azide- and alkyne-containing molecular probe was synthesized and utilized in a “click” chemistry protocol to fluorescently tag potential targets of the hydrazide class of inhibitors. The assay identified a protein of approximately 25 kDa in size that is likely associated with stalled non-stop ribosomal complexes, which may be a hydrazide class target.

Table 1- Hydrazide class inhibitors identified by the high-throughput screen

The screen identified 21 hydrazide inhibitors of *trans*-translation with a variety of chemical side groups

KKL #	HTS Activity *	R ₁	R ₂	R ₃
63	9.4	Ph	H	H
65	10.4	CH ₃	Br	H
139	6.0	Br	H	CH ₃
138	2.5	H	H	CH ₃
137	9.9	OC ₄ H ₉	H	H
141	7.1	OC ₄ H ₉	H	CH ₃
136	11.9	OC ₃ H ₇	H	H
64	1.5	OCH ₃	H	H
140	5.1	OC ₃ H ₇	H	CH ₃
142	3.5	OCH ₂ Ph	H	CH ₃
141	7.1	OC ₄ H ₉	H	CH ₃

KKL #	HTS Activity	R ₄	R ₅
143	3.0	C ₄ H ₉	C ₃ H ₇
150	2.1		
151	1.8		
153	2.4		
148	4.1		
62	6.9		
147	1.1		
149	2.0		
86	4.1		
152	2.0		

* "HTS Activity" indicates the fold-change in luminescence relative to a vehicle control

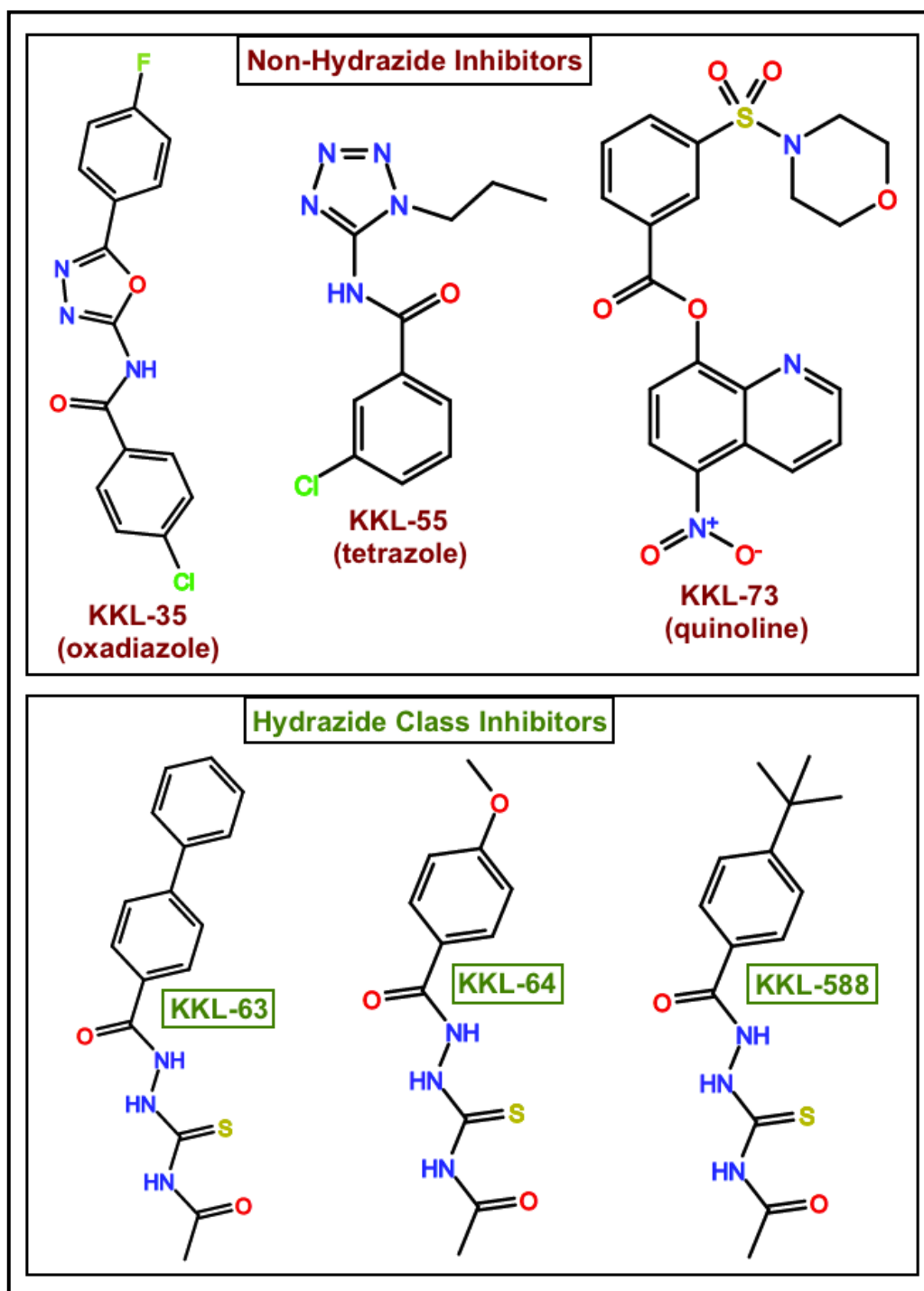


Figure 3- Comparison of hydrazide and non-hydrazide class inhibitors

Previously studied molecules identified by the high-throughput screen include KKL-35, KKL-55, and KKL-73. Hydrazide inhibitors identified by the screen include KKL-63 and KKL-64.

MATERIALS AND METHODS

Reagents, Strains, and Media

All synthetic precursors were obtained from Sigma-Aldrich (St. Louis, MO). All bacterial strains used are from the Keiler Lab strain collection, with the exceptions of *E. coli* $\Delta tolC$ pNS-His (gift from Divya Hosangadi) and *E. coli* *LptD*4213 (gift from Joe Pogliano) (11). Media used for minimum inhibitory concentration (MIC) and other assays for each bacterial strain are shown in Table 2.

Table 2- Media used for different bacterial strains

Bacterial Strain	Media Used
<i>E. coli</i> str. K-12 substr. MG1655 $\Delta tolC$ (<i>E. coli</i> $\Delta tolC$)	Lysogeny Broth (LB)
<i>Bacillus anthracis</i> Sterne	
<i>Shigella flexneri</i> str. 2a2457t (<i>S. flexneri</i>)	
Methicillin Resistant <i>Staphylococcus aureus</i> str. USA300 (MRSA USA300)	
<i>E. coli</i> str. K-12 substr. MG1655 $\Delta tolC$ pNS-His (<i>E. coli</i> $\Delta tolC$ pNS-His)	LB with 30 μ g/mL Kanamycin (LB+Kan)
<i>Mycobacterium smegmatis</i> str. mc ² 155 (<i>M. smegmatis</i>)	LB with 0.2% Tween-80 (LB+Tween)
<i>E. coli</i> str. K-12 substr. MG1655 (<i>E. coli</i>)	Mueller-Hinton Broth (MH)
<i>E. coli</i> str. 101-1	
<i>Acinetobacter baumannii</i>	
<i>Shigella boydii</i>	
<i>Pseudomonas aeruginosa</i>	
<i>Klebsiella pneumoniae</i>	
<i>Haemophilus influenzae</i>	Brain Heart Infusion broth supplemented with 10 μ g/mL hemin and 2 μ g/mL NAD ⁺ (sBHI)

Synthesis of KKL-64

To a solution of 4-methoxybenzhydrazide (500 mg, 3.01 mmol) in methanol (10 mL) was added acetyl isothiocyanate (0.30 mL, 345 mg, 3.41 mmol) at room temperature. An additional 10 mL of methanol was added after 10 minutes. After approximately 14 hours, the precipitated reaction product was isolated by vacuum filtration and washed with methanol (three times, approximately 20 mL each time); washed precipitate was resuspended in hot 100% ethanol (30 mL) and vacuum filtered with 21.7% yield (174.3 mg, 0.652 mmol). The product was verified using thin layer chromatography (TLC) and nuclear magnetic resonance spectroscopy (NMR). ^1H NMR (400 MHz, $\text{DMSO-}d_6$) δ 2.21 (s, 3-H), 3.87 (s, 3-H), 7.06 (d, 2-H), 7.88 (d, 2-H), 10.92 (s, 1-H), 11.59 (s, 1-H).

Synthesis of KKL-588

To a solution of 4-*tert*-butylbenzoic hydrazide (510 mg, 2.65 mmol) in methanol (5 mL) was added acetyl isothiocyanate (0.23 mL, 263 mg, 2.62 mmol) at room temperature. Additional methanol was added at approximately 15 hours. At 29 hours, the precipitated reaction product was isolated by vacuum filtration (three times; filtrate evaporated, resuspended in methanol, and filtered each time) and washed with methanol (three times, approximately 15 mL each time). Filtered product was further purified by silica gel column chromatography using 5% methanol in dichloromethane

(DCM) as a mobile phase with 1.32% yield (9.7 mg, 34.5 μ mol). The product was verified using TLC and NMR. ^1H NMR (400 MHz, CDCl_3) δ 1.30 (s, 3-H), 1.32 (s, 9-H), 7.48 (d, 2-H), 7.82 (d, 2-H), 8.30 (s, 1-H), 10.96 (s, 1-H).

Synthesis of 4-Phenylbenzoic Hydrazide

To a solution of methyl-4-phenylbenzoate (500 mg, 2.36 mmol) in methanol (10 mL) was added hydrazine monohydrate (0.13 mL, 0.134 mg, 2.68 mmol) at 70 $^\circ\text{C}$. The reaction was refluxed for 20 minutes at 72-75 $^\circ\text{C}$ followed by 7 hours 40 minutes at 77-80 $^\circ\text{C}$ and left to cool overnight. Solvent was evaporated and the reaction mixture was dissolved in 5-10% methanol in DCM before purification with silica gel column chromatography using 5% methanol in DCM as a mobile phase with 32.7% yield (163 mg, 0.772 mmol). The product was verified using TLC and NMR. ^1H NMR (400 MHz, CDCl_3) δ 0.91 (d, 2-H), 7.40 (d, 1-H), 7.47 (t, 2-H), 7.61 (d, 2-H), 7.67 (d, 2-H), 7.82 (d, 2-H).

Synthesis of KKL-63

To a solution of 4-phenylbenzoic hydrazide (159 mg, 0.752 mmol) in methanol (20 mL) was added acetyl isothiocyanate (0.09 mL, 104 mg, 1.02 mmol) at room temperature. After 4.5 hours, the precipitated reaction product was isolated by vacuum filtration (two times; filtrate evaporated, resuspended in methanol, and filtered the second time) and washed with methanol (four times, approximately 20 mL each time) with 12.1% yield (28.6 mg, 91.3 μ mol). The product was verified using TLC and NMR.

^1H NMR (400 MHz, CDCl_3) δ 2.23 (s, 3-H), 7.42 (d, 1-H), 7.48 (t, 2-H), 7.63 (d, 2-H), 7.72 (d, 2-H), 7.94 (d, 2-H), 8.40 (s, 1-H), 9.90 (s, 1-H).

Minimum Inhibitory Concentration (MIC) Broth Microdilution Assays

Overnight cultures of bacteria were diluted to $\text{OD}_{600\text{nm}}=0.001$ ($\text{OD}_{600\text{nm}}=0.005$ for *B. anthracis*) in culture media. 50 μL of diluted culture was pipetted into each well of a round-bottom 96-well plate, and an additional 50 μL was pipetted into the top row or left column of the plate. Inhibitors were diluted from dimethyl sulfoxide (DMSO) frozen stocks into the top/left wells. Consecutive 50 μL transfers from the top/left wells of the plate were used to create a series of 2-fold dilutions of each inhibitor. For *M. smegmatis*, sterile water was transferred into the empty space between wells to prevent media evaporation. All 96-well plates were sealed with sterile film before incubation. The MIC for each inhibitor was defined as the well of the lowest calculated inhibitor concentration where no bacterial growth (indicated by lack of turbidity) was visible after an incubation of 24 hours (48 hours for *M. smegmatis*) at 37°C . Vehicle (DMSO) control lanes were used on every 96-well plate to verify compound-specific antibacterial activity.

Combination Activity Checkerboard Assays

Overnight cultures of *E. coli* ΔtolC were diluted in LB to $\text{OD}_{600\text{nm}}=0.001$. Diluted broth was pipetted in 50 μL volumes into the wells of a round-bottom 96-well plate, with an additional 50 μL pipetted into the wells on two edges of the plate. One compound

was added at 4xMIC to the top row of wells on the plate and diluted in a twofold series down the plate columns. Another compound was added to the left column of the plate at 4xMIC and diluted in a twofold series across the plate rows. The plate was sealed with sterile film before incubation. The pattern of visible inhibition of growth (as indicated by lack of turbidity) was recorded after 24 hours of incubation at 37 °C.

To supplement the checkerboard data from the two-fold dilution plates outlined above, additional combinations of different inhibitor concentrations were tested in individual wells of a 96-well plate. These plates were also sealed with sterile film and results were recorded after 24h of incubation at 37 °C.

Click Chemistry Conjugation Assay for Target Identification

5 mL of overnight culture of *E. coli* $\Delta tolC$ or *E. coli* $\Delta tolC$ pNS-His in LB or LB+Kan, respectively, was diluted into 95 mL of culture medium and grown for 4-9 hours at 37°C. The strain containing pNS-His was induced for the final 3 hours of incubation with 1 mM IPTG. Following incubation, the cells were pelleted at 5000 rpm at 4°C using an Allegra F0685 rotor and resuspended in approximately 6% of original culture volume of cold phosphate-buffered saline (PBS; 100 mM Na₂HPO₄, 100 mM NaCl, pH=7.0) with 0.8-1.4 mM PMSF for protease inhibition. The cells were lysed on ice by nine 30-second bursts of sonication using a Branson Sonifier Analog Cell Disruptor, and the lysate was clarified by two 10-minute spins at 14000 rpm at 4 °C using an Allegra F301.5 rotor.

KKL-2101 (synthesized by John Alumasa) or vehicle (DMSO) was added from frozen DMSO stocks to aliquots of the clarified lysate at KKL-2101 concentrations between 0 μ M and 500 μ M, and the aliquots were incubated with agitation at 37 °C for 1-1.5 hours. Lysate aliquots containing KKL-2101 or DMSO vehicle were divided into 100-150 μ L portions in a 96-well plate and cross-linked directly under a UV light for 25 minutes. All cross-linked lysate aliquots were stored at -20°C.

Aliquots of cross-linked lysate (typical volume of 100 μ L used) were denatured by the addition of 0.25 lysate volumes of 10% sodium dodecyl sulfate (SDS) and 0.55 volumes of methanol followed by 5 minutes of incubation at 95 °C. To set up click chemistry reactions, the following reagents were then added to the denatured lysates (in terms of original lysate volume): 0.55 volumes of acetonitrile, 0.06 volumes of KKL-2099 (dansyl azide, synthesized by John Alumasa), 0.01 volumes of 50 mM CuSO₄, 0.05 volumes of 50 mM THPTA, and 0.05 volumes of hydrazine monohydrate. Reactions were incubated in the dark at room temperature for between 1 and 24 hours.

Following incubation, reactions were precipitated by the addition of 1 mL each of cold acetone, then centrifuged at 16,873xg for 10 minutes prior to a wash with an additional 1 mL of cold acetone and an additional 10-minute spin. All acetone-containing supernatants were discarded, and precipitated protein reaction pellets were left open to evaporate any residual solvent. Precipitated reactions were re-solubilized in one original lysate volume of 1x Laemmli SDS Loading buffer by heating at 95 °C and separated using tris-glycine SDS-PAGE prior to viewing on a UVP ultraviolet gel box.

RESULTS

Synthesis of Hydrazide Class Inhibitors

KKL-64 and KKL-588 were successfully synthesized using a one-step scheme with commercially available reagents (Figure 4a,b). This one-step synthesis was accomplished at room temperature with the addition of acetyl isothiocyanate to a solution of a benzoic hydrazide-containing compound. The benzoic hydrazide required for the synthesis of KKL-63, 4-phenylbenzoic hydrazide, was unavailable commercially at an affordable price, and was therefore synthesized from commercially available building blocks (Figure 5). KKL-63 was then synthesized from this product and acetyl isothiocyanate in the same manner as the other hydrazide class inhibitors (Figure 4c). The purity of all compounds was verified by TLC and proton NMR, while the identity of all synthesized compounds was verified by proton NMR (Figure 6). Select impurities were occasionally visible in the proton NMR data (listed as “U.I.” in Figure 6). These may be due to the existence of contaminants in the purified compound stock; however, purity co-verification with TLC and NMR showed no more—and generally far less—than 5% impurity (by visual estimation of TLC spots) in these stocks. Another source of unknown NMR peaks may be the possible reuse of incompletely cleaned NMR tubes and/or caps.

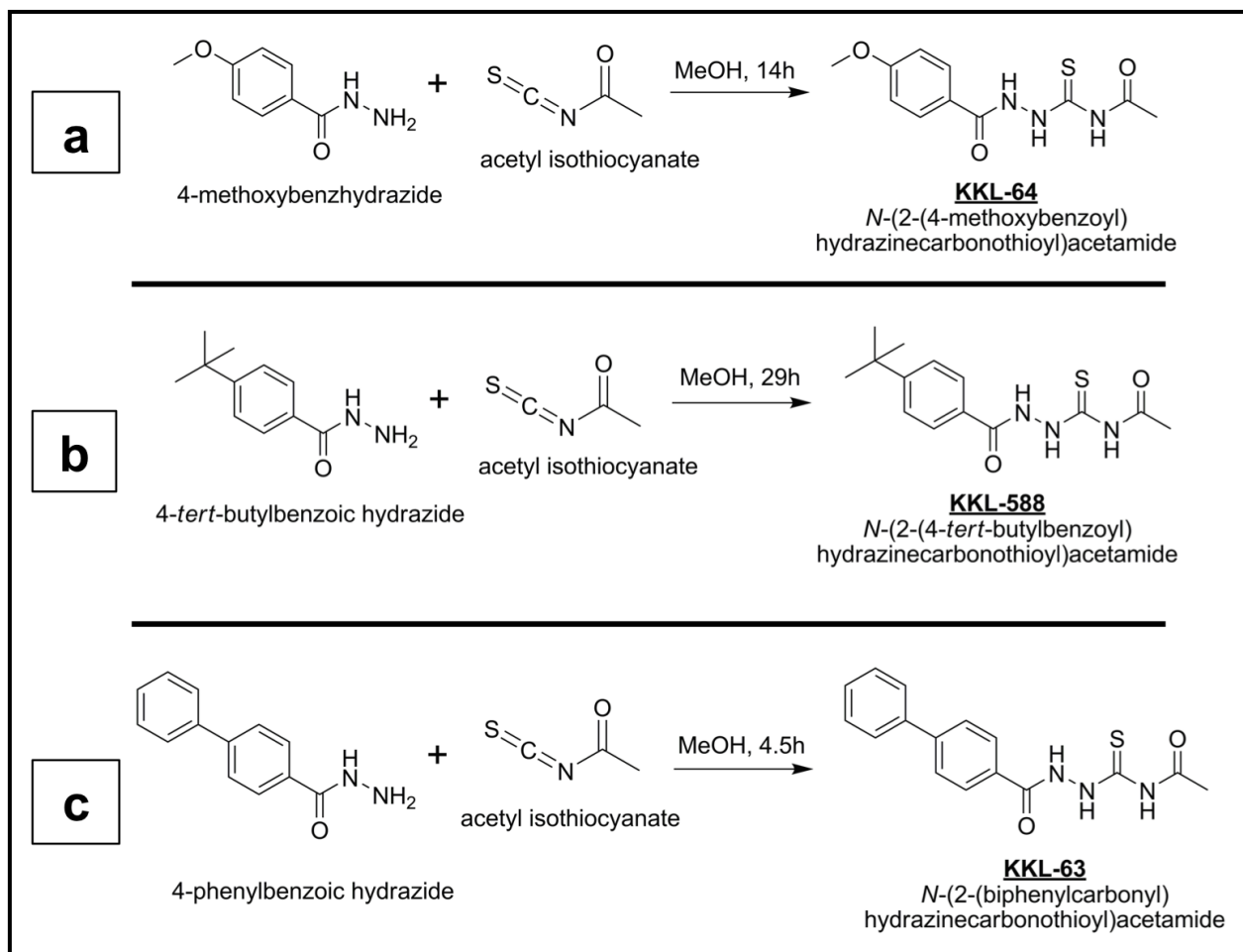


Figure 4- Synthetic schemes for hydrazide class inhibitors

a,b, KKL-64 (**a**) and KKL-588 (**b**) were synthesized using a one-step method with commercially available reagents in methanol. **c**, KKL-63 was synthesized using the same one-step method following the previous synthesis of 4-phenylbenzoic hydrazide.

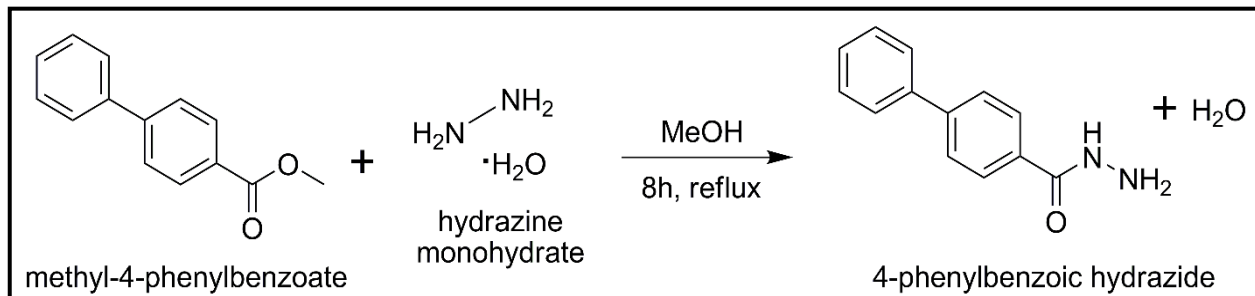


Figure 5- Synthetic scheme for 4-phenylbenzoic hydrazide

To create the benzoic hydrazide precursor for the synthesis of KKL-63, methyl-4-phenylbenzoate was refluxed with hydrazine monohydrate in methanol.

6a

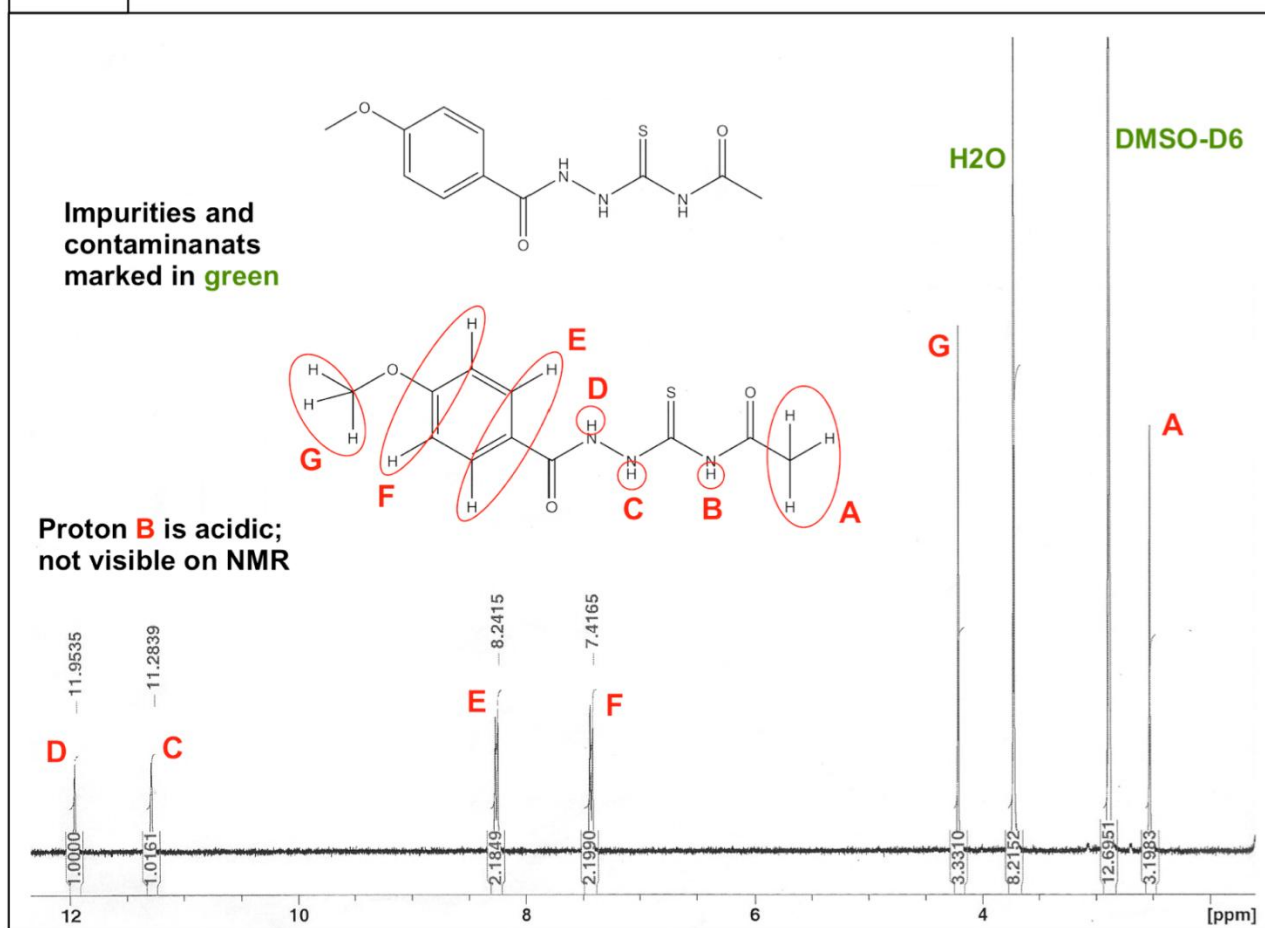
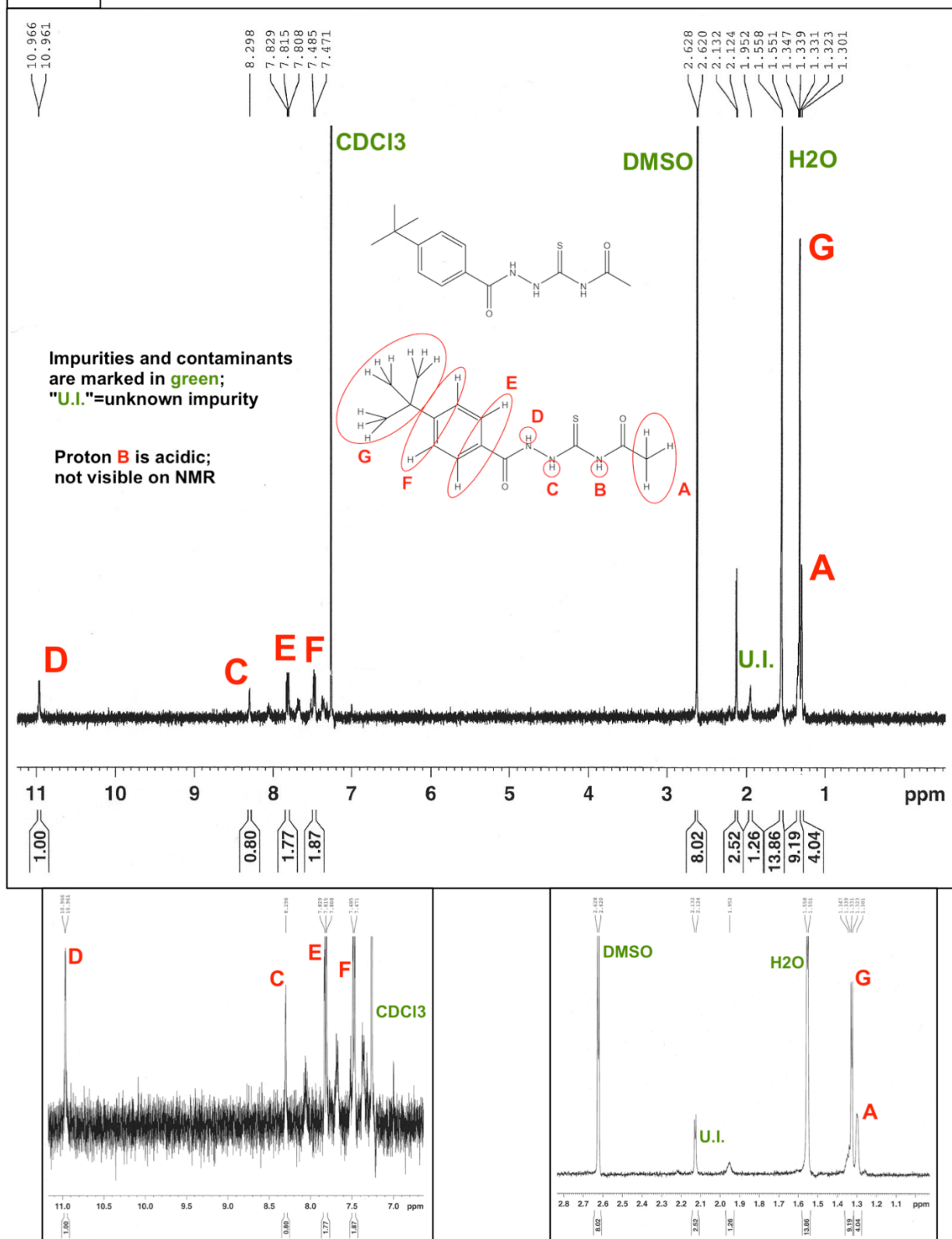
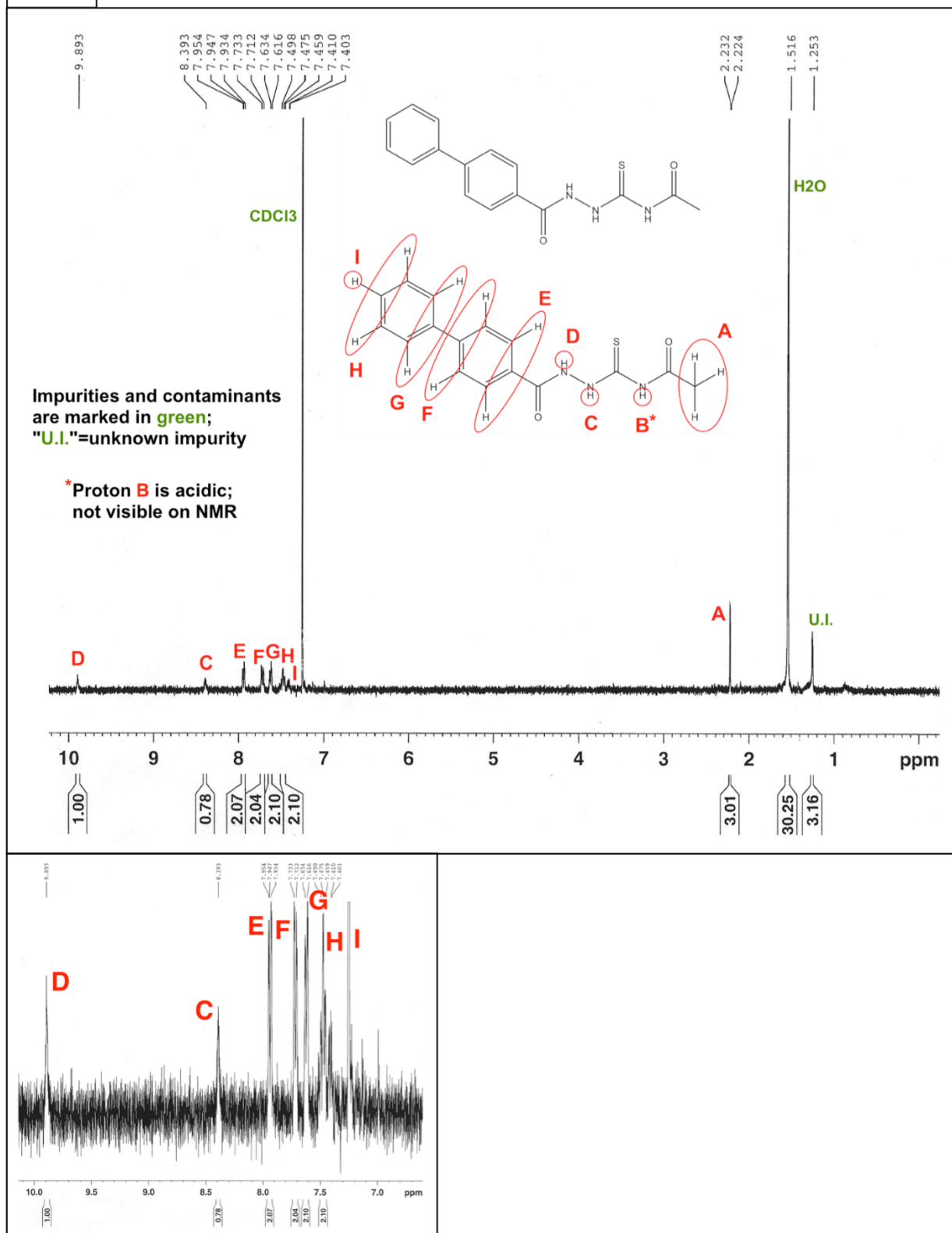


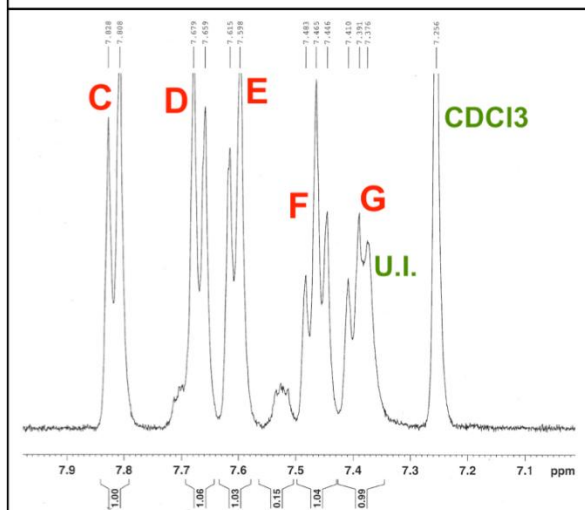
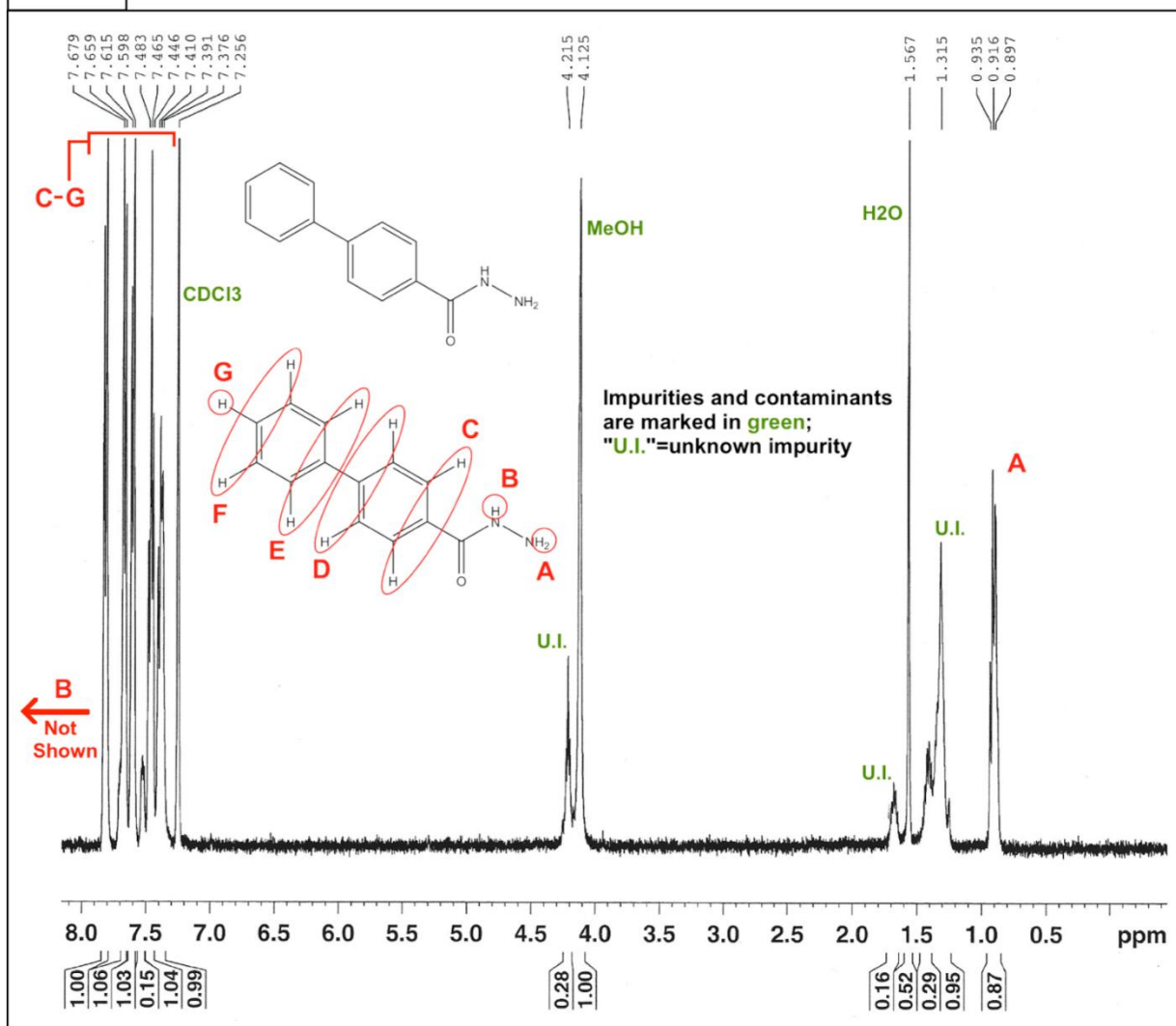
Figure 6- Annotated proton NMR data for synthesized compounds

¹H NMR was used to verify the identity and the purity of all synthesized compounds: KKL-64 (a), KKL-588 (b), KKL-63 (c), and 4-phenylbenzoic hydrazide (d). DMSO-D₆ (a) or CDCl₃ (b-d) was used as the solvent for the NMR readings. Peaks that correlate with the shifts of known hydrogens on synthesized molecules are marked in red, while solvent peaks and impurities are marked in green. In the KKL-64 NMR (a), the shifts shown are ~0.36 ppm downfield of their actual values due to an error in TMS peak alignment. In the 4-phenylbenzoic hydrazide NMR (d), due to an error in zoom the field pictured does not contain one of the known peaks from the synthesized compound. All impurities marked as unknown ("U.I.") are proposed to have arisen either from residual contaminant (<5% by TLC) in the purified compound stocks or from contamination in NMR tubes and/or caps. The proton marked in red as "B" in the hydrazide class compounds (a-c) does not produce a visible peak by NMR due to the electron-poor nature of the nitrogen to which it is bound; this makes the proton highly acidic and leads to its dissociation, which precludes NMR detection.

6b



6c

6d

Hydrazide Class Inhibitors are Effective Antibiotics

Following the synthesis of hydrazide class inhibitors, broth microdilution assays were used to characterize the antibacterial activity of these compounds. These assays revealed MIC values for the compounds KKL-63 and KKL-588 in the low to mid micromolar range in nonpathogenic laboratory bacterial strains (Table 3). The compound KKL-64 exhibited generally higher MIC values for most strains and species, implying a variable structure-activity relationship for this inhibitor class. Similar MIC values were observed for these compounds in some pathogenic strains (Table 4). Several species of gram-negative pathogens, as well as the MG1655 laboratory strain of *E. coli*, were intrinsically resistant to all tested hydrazide-class inhibitors at the highest concentrations used (Tables 3 & 4).

To overcome intrinsic resistance due to efflux pumps or outer membrane impermeability, hydrazide compounds were tested against *E. coli* $\Delta tolC$ —which lacks the channel component of a broad range of efflux systems—and *E. coli* *lptD4213*, which has a very permeable outer membrane due to a mutation in an outer membrane protein involved in lipopolysaccharide trafficking (11). Hydrazide class inhibitors displayed antibacterial activity against both strains, showing that both decreased efflux and increased membrane permeability can lead to increased antibiotic efficacy, and that therefore efflux and/or membrane impermeability likely play a role in the intrinsic resistance of certain gram-negative bacteria to hydrazide class *trans*-translation inhibitors.

Though hydrazide class compounds have been shown to inhibit *trans*-translation in the whole-cell luciferase assay outlined in Figure 2, it was unknown whether these

inhibitors also act on other pathways in the bacterial cell. To test this, the antibacterial activity of hydrazide class inhibitors was assayed against the strain *E. coli* $\Delta tolC$ $\Delta ssrA$, which lacks the gene that codes for tmRNA and therefore does not have a functional *trans*-translation system. Hydrazide class inhibitors displayed antibacterial activity against this strain, and are therefore capable of antibiotic activity through a mechanism other than the inhibition of *trans*-translation (Table 3). The mean MIC values for all hydrazide class inhibitors increased 0.5 to 2.5-fold upon the deletion of *ssrA* from *E. coli* $\Delta tolC$; additional testing is necessary to assess the significance of this result.

Table 3- Mean MIC values for synthesized hydrazide class inhibitors in nonpathogenic bacterial strains

Compound	Minimum Inhibitory Concentration (MIC)**, μ M					
	<i>E. coli</i>	<i>E. coli</i> $\Delta tolC$	<i>E. coli</i> <i>lptD</i> 4213	<i>E. coli</i> $\Delta tolC$ $\Delta ssrA$	<i>Mycobacterium smegmatis</i>	<i>Bacillus anthracis</i> <i>sterne</i>
KKL-63	>100	1.2	50	3.1	25	1.6
KKL-588	>100	4.6	50	12.5	50	3.1
KKL-64	>200	50	n.d.*	75	75	50

*n.d. = value not determined

** All compounds were tested in duplicate or greater measurements and the resultant MIC values were averaged in the table. No inhibitor displayed a greater than twofold variation in MIC between tests.

Table 4- Mean MIC values for synthesized hydrazide class inhibitors in pathogenic bacterial strains

Compound	Minimum Inhibitory Concentration (MIC)*, μ M				
	<i>Haemophilus influenzae</i>	<i>Shigella flexneri</i>	<i>Shigella boydii</i>	MRSA USA300	<i>E. coli</i> 101-1
KKL-63	3.1	>100	12.5	3.1	>100
KKL-588	9.4	>100	50	9.4	>100
KKL-64	25	25	50	50	>200

Compound	Minimum Inhibitory Concentration (MIC)*, μ M			
	<i>Acinetobacter baumannii</i>	<i>Klebsiella pneumoniae</i>	<i>Pseudomonas aeruginosa</i>	<i>Salmonella enterica</i> serovar typhimurium
KKL-63	>100	>100	>100	>100
KKL-588	>100	>100	>100	>100
KKL-64	>200	>200	>200	>200

* All compounds were tested in duplicate or greater measurements and the resultant MIC values were averaged in the table. No inhibitor displayed a greater than twofold variation in MIC between tests (with the exception of KKL-63, which displayed fourfold variation in activity against MRSA USA300)

Combinatorial Activity of Hydrazide Class and Other Inhibitors

To further characterize the hydrazide class inhibitors, the representative compound KKL-64 was tested for antibacterial activity in combination with other known inhibitors of *trans*-translation. Combinatorial activity between two antibiotic compounds can fall into three different classifications: additive, synergistic, or antagonistic. Additive activity is when two antibiotics complement—but do not increase—each others' efficacy. Meanwhile, synergistic activity occurs when one antibiotic makes another more

effective, while antagonistic activity occurs when one antibiotic makes another less effective.

Combinatorial activity can be viewed from the perspective of “proportions of MIC”. This concept is best communicated with an example, in this case regarding two compounds referred to as “antibiotic Θ ” and “antibiotic Σ ”. In a given strain of bacteria, antibiotic Θ has an MIC of 50 μM , while in the same strain antibiotic Σ has an MIC of 3 μM . Therefore, in terms of “proportions of MIC”, 50 μM of Θ would be $1x\text{MIC}_{\Theta}$, 25 μM of Θ would be $0.5x\text{MIC}_{\Theta}$, 12.5 μM of Θ would be $0.25x\text{MIC}_{\Theta}$, and so on. Meanwhile, 3 μM of Σ would be $1x\text{MIC}_{\Sigma}$, 1.5 μM of Σ would be $0.5x\text{MIC}_{\Sigma}$, 0.75 μM of Σ would be $0.25x\text{MIC}_{\Sigma}$, and so on.

In the case of additive activity, the proportions of MIC for two antibiotics that are effective in combination must add to approximately 1. For example, if Θ and Σ are additive, a combination of $0.5x\text{MIC}_{\Theta}$ and $0.5x\text{MIC}_{\Sigma}$ will inhibit bacterial growth (as $0.5+0.5=1$), but a combination of $0.25x\text{MIC}_{\Theta}$ and $0.25x\text{MIC}_{\Sigma}$ will not (as $0.25+0.25=0.5$, which is less than $1x\text{MIC}$). If the two compounds are synergistic, bacterial growth inhibition will be seen even when the proportions of MIC for the two compounds add to less than 1—for example, if $0.05x\text{MIC}_{\Theta}$ and $0.3x\text{MIC}_{\Sigma}$ together inhibit bacterial growth, then the two antibiotics work synergistically ($0.05+0.3=0.35$, which is <1). Antagonistic activity, meanwhile, effectively raises MIC for one compound when the other is present. An example of this would be if $1x\text{MIC}_{\Theta}$ and $0.5x\text{MIC}_{\Sigma}$ failed to inhibit bacterial growth ($1+0.5=1.5$, which is >1).

Visually, combinatory activity can be represented using a 2-dimensional graph, with the proportion of MIC for one antibiotic on the X-axis and the proportion of MIC for

another antibiotic on the Y-axis (Figure 7a). The points plotted represent the lowest combined MICs discovered by combinatory testing. For example, if growth inhibition was observed in a well containing $0.25 \times \text{MIC}_\theta + 0.5 \times \text{MIC}_\Sigma$, but not in wells containing $0.125 \times \text{MIC}_\theta + 0.5 \times \text{MIC}_\Sigma$ or $0.25 \times \text{MIC}_\theta + 0.25 \times \text{MIC}_\Sigma$, then a point would be plotted at $(x=0.25 \times \text{MIC}_\theta, y=0.5 \times \text{MIC}_\Sigma)$ —or, in Cartesian coordinate terms, (0.25,0.5). This is, of course, if more exact concentration combinations were not tested.

A perfectly straight line from the (0,1) point to the (1,0) point represents a perfectly additive pair of antibiotics, where the two compounds must be used at a combined proportion of MIC (i.e. ${}_x\text{MIC}_\theta + {}_x\text{MIC}_\Sigma$) of $1 \times \text{MIC}$ or greater in order to be effective. In the analysis of the hydrazide compound data, a threshold for synergistic activity of $0.5 \times$ combined MIC was used. In real terms, this means that for two antibiotics to be considered “synergistic”, they must be effective when used together at a combined proportion of MICs (i.e. ${}_x\text{MIC}_\theta + {}_x\text{MIC}_\Sigma$) of ≤ 0.5 . In Figure 7a, a perfectly additive plot is represented by the blue line while a synergistic plot is represented by the green line. In order for a pair of antibiotics to be considered synergistic, there must be combinatory MIC points plotted at the green line or closer to the X- and Y-axes than the green line. The threshold for antagonistic antibiotics was not considered for this experiment.

When used in combinatory broth microdilution (“checkerboard”) assays with other antibiotics that inhibit *trans*-translation, the hydrazide class inhibitor KKL-64 exhibited effects that were between additive and near-synergistic in character (Figure 7b). The compounds used in this assay are representative of each major class of *trans*-translation inhibitor: KKL-35 and KKL-10 are members of the oxadiazole class, KKL-55

is a member of the tetrazole class, and KKL-207 is another member of the hydrazide class (synthesis and structure not shown; compound structurally related to KKL-64 with the terminal methoxy group replaced by a fluoride atom).

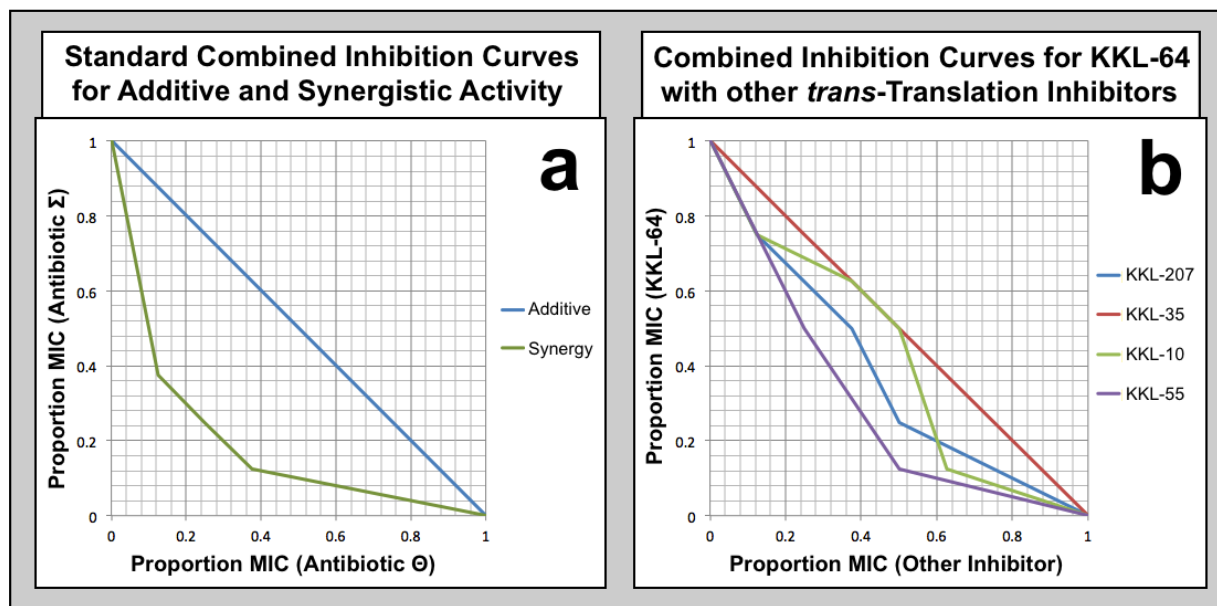


Figure 7- Activity of KKL-64 in combination with other *trans*-translation inhibitors

Inhibitors were tested in combinatory checkerboard assays. **a**, Synergistic activity is defined as a twofold reduction in MIC when two antibiotics are combined, while additive activity is defined as no reduction in MIC when two compounds are combined. **b**, Based on its hydrazide class structure and high similarity to KKL-64, KKL-207 serves as a control for a compound with a similar molecular target and binding site as KKL-64, while KKL-35, KKL-10, and KKL-55 serve to compare KKL-64 with inhibitors of non-hydrazide classes.

Combinatorial activity can lead to insights into the molecular targeting of related antibiotics. Two antibiotics that are additive in nature may be competing for the same inhibitory binding site on a certain protein or RNA molecule, where (as an example) $0.5 \times \text{MIC}_{\Theta}$ and $0.5 \times \text{MIC}_{\Sigma}$ would each bind and inhibit half of the required number of macromolecules for growth inhibition in each bacterial cell. Meanwhile, two antibiotics

that are synergistic in nature are likely binding to different macromolecules, and possibly targeting different pathways or phenotypic cell types.

KKL-207 was used as a positive control for additive activity in this assay, as its close structural relationship to KKL-64 allows one to assume it binds to the same site, albeit with a possibly different affinity. KKL-64 and KKL-207 were near-perfectly additive in nature; the slightly synergistic appearance of their relationship could easily be due to biological variation. Perfectly additive activity was observed between KKL-64 and KKL-35 and near-perfectly additive activity was observed between KKL-64 and KKL-10; meanwhile, close to synergistic activity was observed between KKL-64 and KKL-55. This implies that while the hydrazide class inhibitors may have a different molecular target from the tetrazole class inhibitors, there is some support for a hypothesis that the hydrazide and oxadiazole inhibitors bind the same target in a competing fashion.

Click Chemistry Probe Assay for Hydrazide Inhibitor Targets

In order to identify the molecular target or targets of the hydrazide class inhibitors, a probe assay was designed using “click chemistry” techniques. A small-molecule probe named KKL-2101 containing the hydrazide class substructure bordered by a phenyl azide group and an alkyne group was synthesized (Figure 8a). This probe, when added to a bacterial lysate, is intended to bind to the same macromolecular site(s) as the hydrazide class inhibitors; the phenyl azide group is then activated by ultraviolet light to covalently cross-link to nearby sites on the bound macromolecular target (e.g.

protein or RNA). The mechanism of this crosslinking is the formation of a short-lived nitrene radical, which can be followed by covalent binding to a variety of nearby groups (12). Additionally, the nitrene radical can form other reactive species such as ketenimine or azepinone, which have been shown to crosslink RNA in aqueous environments (13).

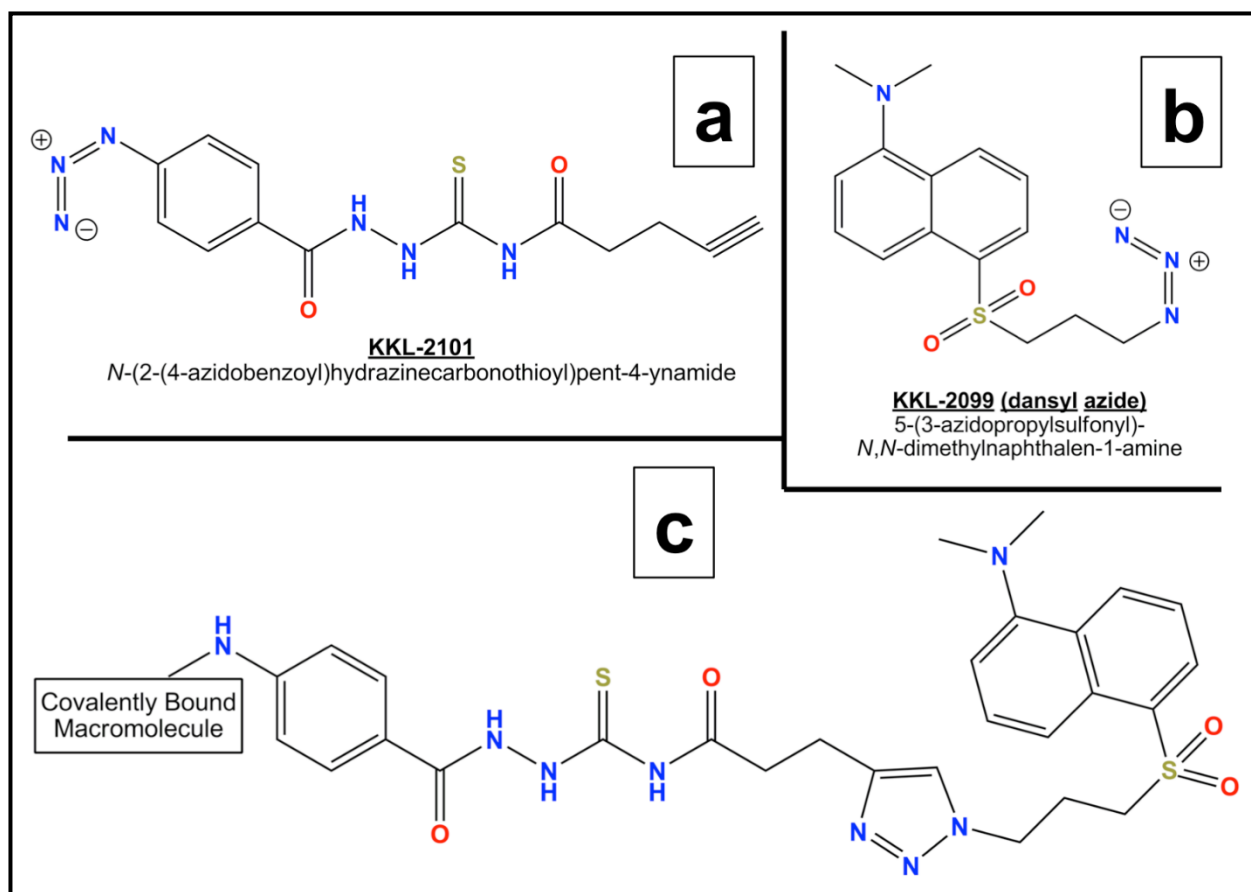


Figure 8- Chemical structures related to the KKL-2101 click probe assay

KKL-2101, (a), contains a phenyl azide group to facilitate covalent crosslinking to proteins or RNA. It also contains the hydrazide class substructure, which allows its specific binding to hydrazide class targets in a bacterial lysate. KKL-2099, (b), contains an azide that can react in a copper-catalyzed “click chemistry” cycloaddition reaction with the alkyne group of KKL-2101, and a dansyl group that is brightly fluorescent during excitation with ultraviolet light. After crosslinking of KKL-2101 and click chemistry with KKL-2099, the resulting structure (c) is a fluorescent tag added covalently to any macromolecule that was originally bound by KKL-2101.

Denaturation of crosslinked lysates then exposes the alkyne group of the KKL-2101 probe to the surrounding solution, allowing a copper-catalyzed “click” cycloaddition of an azide-containing fluorescent marker onto the crosslinked probe (14). This results in a selective covalent linkage of a fluorescent molecule—in this case, a dansyl group from the compound KKL-2099—onto the probe’s macromolecular binding partner or partners (Figure 8b,c).

Following the covalent linkage of a fluorescent group to the possible hydrazide class binding partner(s), the reacted lysates are acetone precipitated, and the isolated proteins are solubilized in Laemmli buffer and separated on a tris-glycine SDS-PAGE gel (Figure 9). Viewing this gel on an ultraviolet light box allows the visualization of all naturally fluorescent and fluorescently tagged proteins in the lysates used for the probe assay. Specifically “bright” bands that appear under ultraviolet light and are present only in samples containing crosslinked probe (not in samples containing a vehicle control) are likely to be specific binding partners of KKL-2101 and—in accordance with the design of the probe—the entire hydrazide class of trans-translation inhibitors. Proteins that specifically bind members of the hydrazide class can then be studied more extensively as potential molecular target(s) of this class.

Lysates from *E. coli* $\Delta tolC$ and *E. coli* $\Delta tolC$ pNS-His were used in the KKL-2101 click assay. *E. coli* $\Delta tolC$ was selected due to the susceptibility of this strain to growth inhibition by the hydrazide class of inhibitors; this susceptibility indicates the presence of a molecular target for the hydrazide class. The strain *E. coli* $\Delta tolC$ pNS-His was

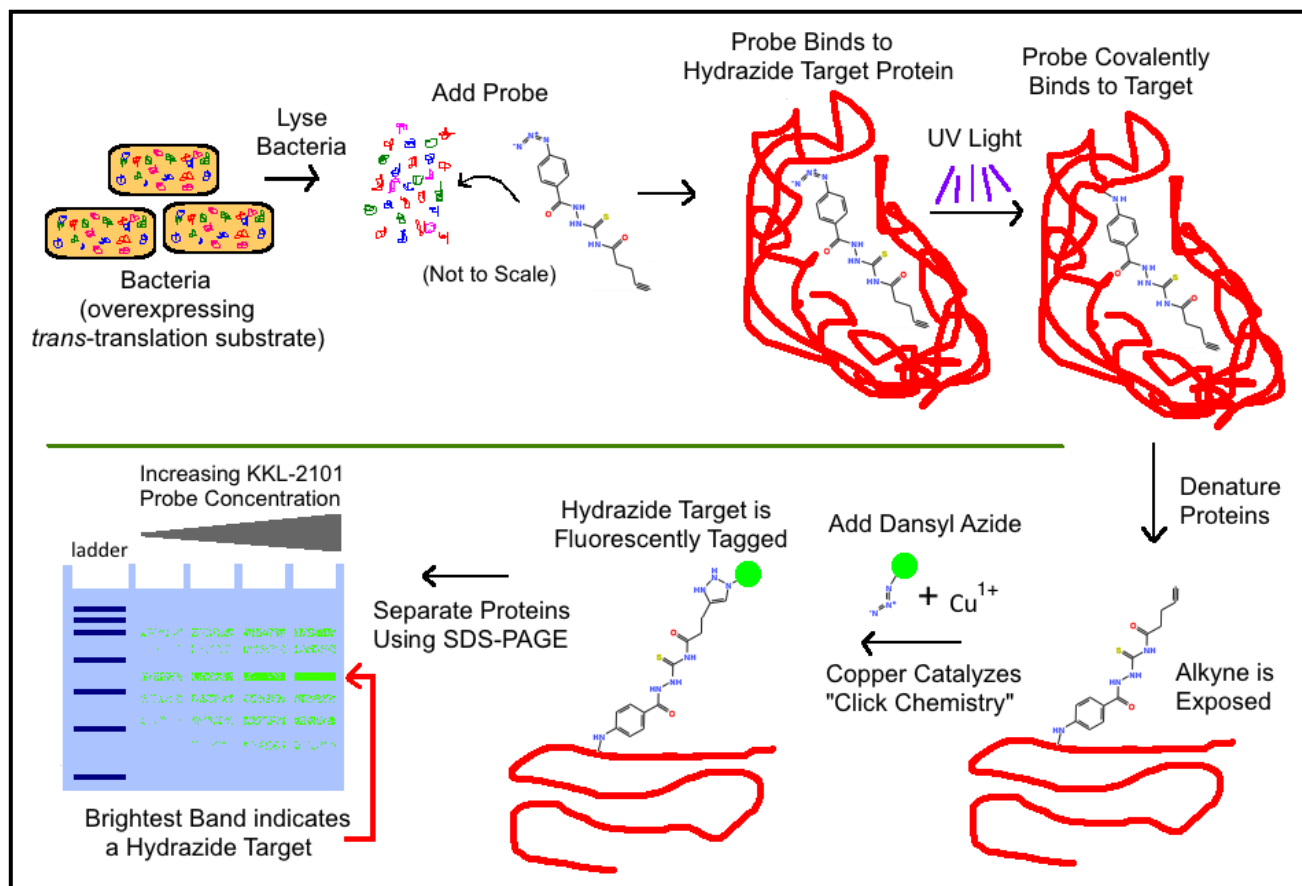


Figure 9- Click chemistry assay for the binding of the KKL-2101 hydrazide probe to target protein(s)

A culture of *E. coli* $\Delta tolC$ or IPTG-induced *E. coli* $\Delta tolC$ pNS-His is lysed by sonication and the lysate is clarified. KKL-2101 or a vehicle control is added to the lysate, which is incubated at 37°C to allow the KKL-2101 probe to bind to potential hydrazide target(s). Ultraviolet light is used to covalently crosslink the probe to the target macromolecule(s), after which the crosslinked lysate is subjected to denaturing conditions to expose the alkyne group of KKL-2101. Reagents for the click chemistry cycloaddition of KKL-2099 (dansyl azide) onto the alkyne portion of macromolecule-bound KKL-2101 are added and the reaction is allowed to proceed. Proteins are isolated by acetone precipitation and separated using SDS-PAGE. Proteins with bound KKL-2101/KKL-2099 complex are brighter under UV illumination than the background proteins of the lysate, and are identified as potential targets for the hydrazide class of *trans*-translation inhibitors.

selected because of its maintenance of an IPTG-inducible plasmid overexpressing nonstop transcripts encoding N-terminally His-tagged peptides. The induction of this strain with IPTG results in a buildup of stalled non-stop ribosomal complexes, which are a hypothesized target for the oxadiazole class *trans*-translation inhibitors. Given the results of the combinatory activity assays—which suggested a common target for the hydrazide and oxadiazole classes of compounds—it was predicted that overexpression of stalled non-stop ribosomal complexes would increase the availability of hydrazide class targets in the *E. coli* $\Delta toIC$ lysate. This would then increase the fluorescent signal of the hydrazide class-binding protein(s) on the final SDS-PAGE gel under ultraviolet illumination.

The KKL-2101 probe was incubated with the *E. coli* $\Delta toIC$ and *E. coli* $\Delta toIC$ pNS-His at titrated concentrations between 0 μ M and 500 μ M prior to crosslinking. Click cycloaddition of KKL-2099 was performed under identical conditions for each lysate sample. Separation of post-reaction lysate proteins on an SDS-PAGE gel showed significant background fluorescence at all concentrations of KKL-2101 as well as in the vehicle control (Figure 10). Increased general fluorescence, likely due to nonspecific binding of KKL-2101, was seen at 200 μ M and 500 μ M KKL-2101. There were no apparent bands apart from those associated with nonspecific binding in the click-treated lysates from *E. coli* $\Delta toIC$ (gel containing all titrated samples from this strain is not shown; 200 μ M sample from *E. coli* $\Delta toIC$ is visible in the far right lane in Figure 10).

The post-click lysates from *E. coli* $\Delta toIC$ pNS-His showed only background fluorescence when crosslinked with 0-20 μ M KKL-2101 (Figure 10, lanes marked “0” through “20”). General increases in fluorescence due to likely nonspecific probe binding

were observed at 200 μ M and 500 μ M KKL-2101 (Figure 10, lanes marked “200” and “500”). At 50 μ M and 100 μ M KKL-2101, no increase in background fluorescence due to likely nonspecific binding was present; however, a brighter band not visible at lower probe concentrations was apparent at approximately 25 kDa (Figure 10, lanes marked “50” and “100”). This band maintained a high relative intensity with increased probe concentration from 50 μ M to 500 μ M KKL-2101. The presence of this band at a concentration where no other probe binding was evident indicates that it represents a specifically bound protein partner of KKL-2101, and therefore a potential target for the hydrazide class of *trans*-translation inhibitors.

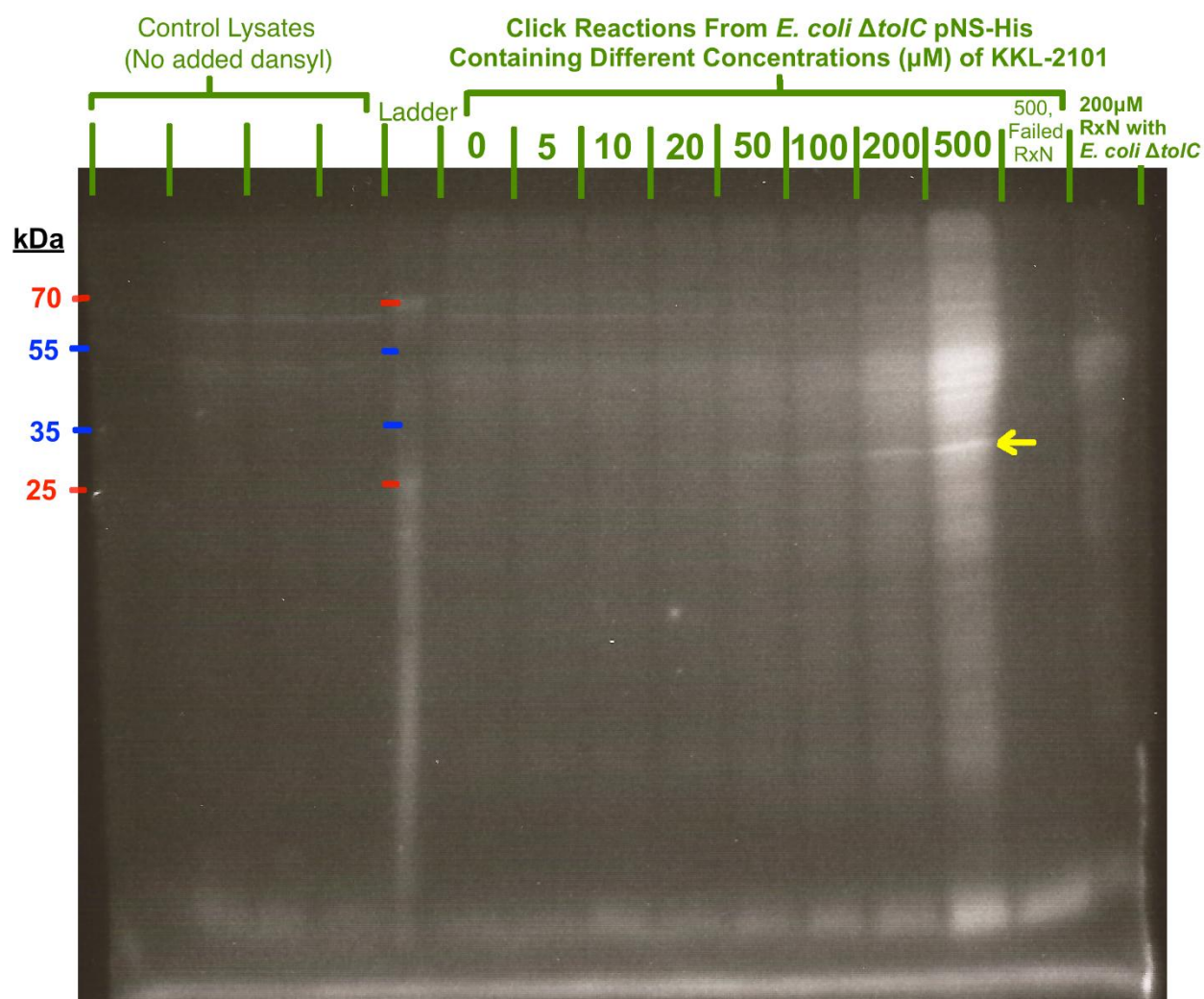


Figure 10- UV illuminated gel with KKL-2101 probed samples

Lysates from *E. coli* $\Delta tolC$ pNS-His were incubated with the KKL-2101 hydrazine class probe, then crosslinked with ultraviolet light and exposed to KKL-2099 (dansyl azide) in click chemistry-catalyzing conditions. The pictured gel shows the separated lysate proteins following the click reaction, illuminated on an ultraviolet light box to visualize fluorescently tagged probe-bound proteins. The yellow arrow indicates the ~25 kDa protein of interest that appears only in lysates from the strain containing pNS-His.

DISCUSSION

The hydrazide class of *trans*-translation inhibitors has not been extensively studied due to the lack of availability of these compounds. In the above results, the one-step synthesis of multiple hydrazide class inhibitors including KKL-64 and KKL-588 is shown. This synthetic method allows for the rapid production of large amounts of compound from commercially available precursors, without the use of harsh solvents or expensive equipment. This synthetic scheme is also adaptable to the synthesis of compounds for which one of the precursors is not commercially available, as seen in the two-step synthesis of KKL-63.

A long-term issue may arise regarding the relatively low yields from the synthesis of hydrazide class inhibitors (ranging from 1.32% to 21.7%). A potential solution to this problem is an alteration in the purification strategy for the hydrazide class compounds, as vacuum filtration can lead to the loss of significant amounts of compound during wash steps. The exclusive use of silica gel column chromatography, which was shown to be an effective secondary purification strategy following the synthesis of KKL-588, could allow the recovery of much more product and starting material following synthesis.

Broth microdilution assays showed that the hydrazide class inhibitors KKL-63, KKL-588, and KKL-64 are effective antibiotics against several pathogenic and nonpathogenic species. The efficacy of these compounds against *S. aureus* and *Shigella* spp. is especially significant given the alarm surrounding resistant strains of these pathogens (2). Additionally, the ability of these compounds to inhibit the growth of

M. smegmatis is promising in their potential use against the related microbial cause of tuberculosis, which poses a widespread and growing threat due to the dual specters of drug resistance and HIV co-infection (15).

One source of some concern is the failure of the hydrazide-class inhibitors to prevent the growth of several gram-negative species of pathogenic bacteria. These species include *Pseudomonas aeruginosa*, *Klebsiella pneumoniae*, *Acinetobacter baumannii*, *Salmonella enterica* serovar Typhimurium, and wild-type and pathogenic *E. coli*, all of which are either discussed in the 2013 WHO Report on Antimicrobial Resistance or are members of the infamous ESKAPE group of multidrug-resistant hospital-associated pathogens (1,16).

Of note is that the resistant phenotype of wild-type *E. coli* is reversed upon the deletion of *toIC*, a gene that encodes the channel portion of many multidrug efflux pumps. It is also partially reversed by the *lptD4213* mutation, which increases outer membrane permeability (11). These results suggest that the hydrazide-resistant phenotype of certain gram-negative pathogens may be due to the efflux of hydrazide class inhibitors by multidrug efflux pumps. Indeed, the hydrazide-resistant pathogenic species mentioned above have all been known to use multidrug efflux as a clinically relevant mechanism of resistance (17-20). Fortunately, there has been some reported development in field of bacterial efflux pump inhibitors (EPIs), and there may be hope for a combination therapy approach using hydrazide class *trans*-translation inhibitors with EPIs in a clinical setting to treat diseases caused by these intrinsically resistant pathogens (21,22).

Although the hydrazide class compounds are being investigated as inhibitors of *trans*-translation, their efficacy in a strain of *E. coli* lacking tmRNA (*E. coli* $\Delta tolC \Delta ssrA$) indicates that they have a secondary target in the bacterial cell when *trans*-translation is not active. It has been hypothesized that various classes of *trans*-translation inhibitors can inhibit so-called “backup” mechanisms for *trans*-translation, which can resolve ribosomal complexes in species of bacteria where *trans*-translation is non-essential. These backup mechanisms include ArfA- and ArfB-mediated ribosome rescue (23 & 24). The proposed binding of hydrazide class compounds to stalled non-stop ribosomal complexes, which are substrates not only for *trans*-translation but also for all known backup mechanisms of ribosome rescue, is in agreement with the hypothesized activity of these compounds against backup mechanisms. The higher apparent MICs for the hydrazide compounds in the tmRNA-deficient strain of *E. coli*—the significance of which may be confirmed with further testing—indicates that their inhibition of *trans*-translation in this species might be more effective than their inhibition of ArfA-mediated ribosome rescue, which is the primary backup mechanism for *trans*-translation in *E. coli* (25).

Meanwhile, combinatory broth microdilution assays showed that the KKL-64 hydrazide-class inhibitor has near-perfectly or perfectly additive effects in combination with oxadiazole class *trans*-translation inhibitors, but an almost synergistic effect in combination with a tetrazole class *trans*-translation inhibitor. Given that two inhibitors with overlapping binding sites on the same molecular target would hypothetically be additive when used in combination, these data align with the hypothesis that the tetrazole class inhibitor KKL-55 targets the protein EF-Tu, while the oxadiazoles have a distinct mechanism of action characterized by direct binding to the stalled non-stop

ribosomal complex. This hypothesis applies to the hydrazide class of inhibitors by suggesting the non-stop complex as a potential molecular target for these compounds.

To further characterize the molecular targeting of the hydrazide class of inhibitors, a click chemistry-based assay using the KKL-2101 molecular probe was designed and carried out. By limiting the bulk of the side groups on the hydrazide molecular probe, this approach was designed to provide a greater chance of on-target binding by KKL-2101. Additionally, the covalent crosslinking step of the assay allowed the complete denaturation of all protein and RNA molecules in the cell after probe binding, meaning that the fluorescent tagging of the alkyne portion of KKL-2101 would proceed even if the hydrazide class of inhibitors binds deep within a large macromolecular structure such as the stalled non-stop ribosomal complex.

Though the KKL-2101 click assay did not indicate that the hydrazide probe binds specifically to any proteins in a lysate of *E. coli* $\Delta tolC$, it did show specific binding of KKL-2101 to a protein of approximately 25 kDa in a lysate of IPTG-induced *E. coli* $\Delta tolC$ pNS-His. This strain was designed to overexpress non-stop transcripts for purification purposes. That the specific binding of KKL-2101 to a lysate protein is unique to this strain as opposed to standard *E. coli* $\Delta tolC$ lysate indicates that the overexpression of stalled non-stop ribosomal complexes increases available binding partners for KKL-2101. Given the structural similarity of KKL-2101 to the hydrazide class of *trans*-translation inhibitors and the likelihood that high-affinity binding partners of an antibiotic are molecular targets for the drug, it appears that the hydrazide class of inhibitors may be targeting a protein of ~25 kDa in size in the stalled non-stop ribosomal complex.

There are certainly several proteins of approximately this size in the bacterial ribosome, including the proteins S2, S3, S4, L1, L2, L3, and L4 (26).

Further studies using the KKL-2101 probe may now be done to validate the results found using the KKL-2101 click experiment. If the ~25 kDa protein is confirmed to be a high-affinity binding partner for KKL-2101, its identity may be determined through the use of mass spectrometry. Biochemical assays and crystallization with the most effective hydrazide-class compounds would then be good candidates for the confirmation of the identity of this protein as the hydrazide class molecular target. Positive identification of the target of the hydrazide class compounds would further their progress towards clinical trials and eventual human therapeutic use.

REFERENCES

1. **Davies, J., and D. Davies.** 2010. Origins and Evolution of Antibiotic Resistance. *Microbiol. Mol. Biol. Rev.* **74**:417-433
2. **Cadman, H., and L. Martinez, ed.** 2014. Antimicrobial Resistance: Global Report on Surveillance. World Health Organization, Geneva, Switzerland.
3. **Thibonnier, M., Thiberge, J-M., and H. De Reuse.** 2008. Trans-Translation in *Helicobacter pylori*: Essentiality of Ribosome Rescue and Requirement of Protein Tagging for Stress Resistance and Competence. *PLoS ONE* **3**: e3810.
4. **Huang, C., Wolfgang, M.C., Withey, J., Koomey, M., and D.I. Friedman.** 2000. Charged tmRNA but not tmRNA-mediated proteolysis is essential for *Neisseria gonorrhoeae* viability. *EMBO J.* **19**:1098-1107.
5. **Ramados, N.S., Zhou, X., and K.C. Keiler.** 2013. tmRNA is essential in *Shigella flexneri*. *PLoS ONE* **8**:e57537.
6. **Keiler, K.C., and H.A. Feaga.** 2014. Resolving Nonstop Translation Complexes is a Matter of Life and Death. *J. Bacteriol.* **196**:2123-2130.
7. **Keiler, K.C.** 2008. Biology of trans-Translation. *Annu. Rev. Microbiol.* **62**:133-151.
8. **Mehta, P., Richards, J., and A.W. Karzai.** 2006. tmRNA determinants required for facilitating nonstop mRNA decay. *RNA* **12**:2187-2198.
9. **Choy, J.S., Aung, L.L., and A.W. Karzai.** 2007. Lon Protease Degrades Transfer-Messenger RNA-Tagged Proteins. *J. Bacteriol.* **189**:6564-6571.

10. **Ramadoss, N.S., Alumasa, J.N., Cheng, L., Wang, Y., Li, S., Chambers, B.S., Chang, H., Chatterjee, A.K., Brinker, A., Engels, I.H., and K.C. Keiler.** 2013. Small molecule inhibitors of *trans*-translation have broad-spectrum antibiotic activity. Proc. Natl. Acad. Sci. USA **110**:10282-10287
11. **Nonejuie, P., Burkart, M., Pogliano, K., and J. Pogliano.** 2013. Bacterial cytological profiling rapidly identifies the cellular pathways targeted by antibacterial molecules. Proc. Natl. Acad. Sci. USA **110**:16169-16174.
12. **Poe, R., Schnapp, K., Young, M. J. T., Grayzar, J., and M. S. Platz.** 1992. Chemistry and kinetics of singlet (pentafluorophenyl)nitrene. J. Am. Chem. Soc. **114**:5054-5067.
13. **Buchmueller, K. L., Hill, B. T., Platz, M. S., and K. M. Weeks.** 2003. RNA-tethered phenyl azide photocrosslinking via a short-lived indiscriminant electrophile. J. Am. Chem. Soc. **125**:10850-10861.
14. **Rostovtsev, V.V., Green, L.G., Fokin, V.V., and K.B. Sharpless.** 2002. A Stepwise Huisgen Cycloaddition Process: Copper(I)-Catalyzed Regioselective “Ligation” of Azides and Terminal Alkynes. Angew. Chem. Int. Ed. Engl. **41**:2596-2599.
15. **Günther, G.** 2014. Multidrug-resistant and extensively drug-resistant tuberculosis: a review of current concepts and future challenges. Clin. Med. **14**:279-285.
16. **Pendleton, J. N., Gorman, S. P., Whale, W., and B. F. Gilmore.** 2013. Clinical relevance of the ESKAPE pathogens. Expert Rev. Anti infect. Ther. **11**:297-308.
17. **Poole, K., and R. Srikumar.** 2001. Multidrug Efflux in *Pseudomonas aeruginosa*: Components, Mechanisms and Clinical Significance. Curr. Top. Med. Chem. **1**:59-71

18. **Padilla, E., Llobet, E., Doménech-Sánchez, A., Martínez-Martínez, L., Bengoechea, J. A., and S. Albertí.** 2010. *Klebsiella pneumoniae* AcrAB efflux pump contributes to antimicrobial resistance and virulence. *Antimicrob. Agents Chemother.* **54**:177-183.
19. **Wieczorek, P., Sacha, P., Hauschild, T., Zórawski, M., Krawczyk, M., and E. Tryniszewska.** 2008. Multidrug resistant *Acinetobacter baumannii*--the role of AdeABC (RND family) efflux pump in resistance to antibiotics. *Folia Histochem. Cytobiol.* **46**:257-267.
20. **Piddock, L. J. V., White, D. G., Gensberg, K., Pumbwe, L, and D. J. Griggs.** 2000. Evidence for an efflux pump mediating multiple antibiotic resistance in *Salmonella enterica* serovar Typhimurium. *Antimicrob. Agents Chemother.* **44**:3118-3121.
21. **Nakayama, K., Y. Ishida, M. Ohtsuka, H. Kawato, K. Yoshida, Y. Yokomizo, S. Hosono, T. Ohta, K. Hoshino, H. Ishida, K. Yoshida, T. E. Renau, R. Léger, J. Z. Zhang, V. J. Lee, and W. J. Watkins.** 2003. MexAB-OprM-Specific Efflux Pump Inhibitors in *Pseudomonas aeruginosa*. Part 1: Discovery and Early Strategies for Lead Optimization. *Bioorg. Med. Chem. Lett.* **13**:4201-4204.
22. **Yoshida, K., Nakayama, K., Ohtsuka, M., Kuru, N., Yokomizo, Y., Sakamoto, A., Takemura, M., Hoshino, K., Kanda, H., Nitantai, H., Namba, K., Yoshida, K., Imamura, Y., Zhang, J.Z., Lee, V.J., and W.J. Watkins.** 2007. MexAB-OprM specific efflux pump inhibitors in *Pseudomonas aeruginosa*. Part 7: highly soluble and in vivo active quaternary ammonium analogue D13-9001, a potential preclinical candidate. *Bioorg. Med. Chem. Lett.* **15**:7087-7097.

23. **Chadani, Y., Ono, K., Ozawa, S., Takahashi, Y., Takai, K., Nanamiya, H., Tozawa, Y., Katsukake, K., and T. Abo.** 2010. Ribosome rescue by *Escherichia coli* ArfA (YhdL) in the absence of *trans*-translation system. *Mol. Microbiol.* **78**:796-808.
24. **Feaga, H. A., Viollier, P. H., and K. C. Keiler.** 2014. Release of nonstop ribosomes is essential. *mBio* **5**:e01916-14.
25. **Chadani, Y., Ono, K., Kutsakake, K., and T. Abo.** 2011. *Escherichia coli* YaeJ protein mediates a novel ribosome-rescue pathway distinct from SsrA- and ArfA-mediated pathways. *Mol. Microbiol.* **80**:772-785.
26. **Stelzl, U., Connell, S., Nierhaus, K. H., and B. Wittman-Liebold.** 2001. Ribosomal proteins: role in ribosomal functions, p.1-12. *In* Encyclopedia for the Life Sciences, Nature Publishing Group.

Gregory H. Babunovic—Academic Vita

85 Minerva Ave.

Hawthorne, NJ 07506

C: (201)401-4989

ghbabunovic@gmail.com

Education

B.S. in Microbiology

B.S. in Immunology and Infectious Disease

The Pennsylvania State University, University Park, PA

Expected Graduation of May 2015

Schreyer Honors Scholar

Research and Related Positions

The Keiler Lab at Penn State

Undergraduate Research Student, August 2012-Present

- Performed thesis work in the identification, synthesis, and characterization of novel antibiotics specific to the *trans*-translation pathway in bacteria

The Khazaie Lab at the Mayo Clinic

Summer Undergraduate Research Fellowship Student, May-August 2014

- Led projects linking mast cell protease expression and purinergic signaling with colon cancer progression

Penn State Department of Biochemistry and Molecular Biology

Teaching Assistant, January-May 2014

- Facilitated experimental design, data analysis, and student discussion in a concept-focused microbiology laboratory

Honors and Awards

Daniel R. Tershak Memorial Scholarship in Molecular and Cell Biology

Awarded by the Penn State Eberly College of Science, July 2014

Second Team Academic All-American

Awarded by the American Collegiate Rowing Association, May 2014

Peter T. Luckie Award for Excellence in Research by a Junior

Awarded by Penn State chapter of Phi Kappa Phi, April 2014

Dr. Keith V. Rohrbach and Dr. Sharon Rohrbach Scholarship

Awarded by the Penn State Eberly College of Science, July 2013

Charles Grier Award for Summer Research Funds

Awarded by the Penn State Department of Biochemistry and Molecular Biology, March 2013

Robert Patterson Endowed Scholarship

Awarded by the Penn State Alumni of Northern New Jersey, August 2011

Eagle Scout

Awarded by the Boy Scouts of America, November 2010

Posters Presented

Efficacy and Molecular Targeting of Hydrazide Class *trans*-Translation Inhibitors

Penn State Undergraduate Exhibition, April 2015

Investigating the Role of Mast Cells in the Development of Colorectal Cancer

Mayo Clinic SURF Poster Session, July 2014

Synthesis and Characterization of a Novel Class of *trans*-Translation Inhibitors

Penn State Undergraduate Exhibition, April 2014

Searching for Molecular Targets of the KKL-55 *trans*-Translation Inhibitor in *Mycobacterium smegmatis*

Penn State Undergraduate Exhibition, April 2013

Relevant Coursework

Current Topics in Immunology

VB SC 448W, Scheduled Spring 2015

Bacterial Pathogenesis

VB SC 418, Scheduled Spring 2015

Medical Microbiology

MICRB 412, Scheduled Spring 2015

Laboratory in Molecular immunology

MICRB 447, Scheduled Spring 2015

Epidemiology of Infectious Diseases

VB SC 444, Scheduled Spring 2015

Honors Independent Research

BMB 496H, Spring 2014 – Spring 2015

Communities of Practice in Biochemistry and Molecular Biology

BMB 488, Spring 2013 – Spring 2015

Bacterial Physiology and Structure

MICRB 401, Fall 2014

Laboratory in Molecular Genetics

BMB 445W, Fall 2014

Laboratory in Proteins, Nucleic Acids, and Molecular Cloning

BMB 442, Fall 2014

Technical Writing

ENGL 202C, Fall 2014

Advanced immunology: Signaling in the immune System

VB SC 432, Spring 2014

General Virology: Bacterial and Animal Viruses

MICRB 415, Spring 2014

Immunological Mechanisms of Vaccination

VB SC 497B, Spring 2014

Honors Biochemistry

BMB 401H and 402H, Fall 2013 – Spring 2014

Physical Chemistry with Biological Applications

BMB 428, Fall 2013

Laboratory of General and Applied Microbiology

MICRB 421W, Fall 2013

Molecular Biology of the Gene

BMB 400, Fall 2013

Honors Principles of Immunology

MICRB 410H, Fall 2013

Independent Research

BMB 496, Spring 2013 – Fall 2013

Laboratory in Organic Chemistry

CHEM 213, Spring 2013

Genetic Analysis

BIOL 322, Spring 2013

Molecular and Cell Biology

BMB/MICRB 251 and 252, Fall 2012 – Spring 2013

Introductory Physics

PHYS 250 and 251, Fall 2012 – Spring 2013

Organic Chemistry

CHEM 210 and 212, Fall 2012 – Spring 2013

Introductory Microbiology

MICRB 201, Fall 2012

Introductory Microbiology Laboratory

MICRB 202, Fall 2012

Antibiotics—Development and Research

BMB 498A, Fall 2012

Calculus and Biology II

MATH 141B, Spring 2012

Experimental Chemistry II—Bioscience

CHEM 113B

Chemical Principles

CHEM 110 and 112, Fall 2011 – Spring 2012

Mechanisms of Disease

VB SC 050S, Fall 2011

Organizations and Service

Penn State Crew

August 2011 – Present

Equipment Manager August – December 2014

Safety Chair March 2014 – August 2014

- Rowed competitively on the national collegiate level at events such as the Head of the Charles Regatta, the Dad Vail Regatta, and the ACRA National Club Championships
- Maintained a rigorous practice and race schedule of approximately 15-30 hours/week
- Served as equipment manager for a fleet of boats with a value greater than \$100,000

Penn State Helping Across the Community

September 2011 – May 2013

Secretary and Housing Chair, May 2012 – May 2013

- Lived in a service-oriented dormitory community with rigorous membership requirements
- Kept track of service hours and housing eligibility for over 30 members, organized club events, and maintained detailed club records as secretary and housing chair

Employment

Ski Campgaw Mountain; Mahwah, NJ

Ski instructor, Winters 2008 – 2014

- Instructed over 200 private and group lessons as a member of the ski school staff
- Assisted managers in the training and assessment of new instructors

Floodwood Mountain Scout Reservation; Lake Clear, NY

Voyageur, Summers 2012-Present

Voyageur in Training, Summers 2009 – 2011

- Guided groups of 4-10 scouts each week between the ages of 12 and 20 on canoe trips of approximately 50 miles
- Carried responsibility for the safety of the scouts and the protection of the Adirondack wilderness through action and education